AN INVESTIGATION OF FRICTION AND WEAR MECHANISMS IN SELECTED THERMOPLASTICS

by

Joseph R. Potter, III

Thesis submitted to the Faculty of the
Virginia Polytechnic Institute and State University
in partial fulfillment of the requirements for the degree of
MASTER OF SCIENCE

in

Mechanical Engineering

Dr. N. S. Eiss. Jr.

Dr. M. Furey

Dr. D. Dwight

August, 1983

Blacksburg, Virginia

AN INVESTIGATION OF FRICTION AND WEAR MECHANISMS IN SELECTED THERMOPLASTICS

by

Joseph R. Potter, III

(ABSTRACT)

These studies developed from Scanning Electron Microscope (SEM) observations of abrasive wear of a polymer disk sliding against metal asperity models. The investigator was unable to observe actual particle formation, but did identify elastic and plastic deformation of the polymer, and a debris buildup and extrusion process occurring at the leading edge of the asperity.

On the assumption that this process could lead to a surface fatigue condition, pin-on-disk wear trials were completed using a spherical steel ball sliding on polycarbonate, rigid PVC, and ultra high molecular weight polyethylene specimens in dry and lubricated conditions. A delay in debris formation was observed in the rigid PVC and polycarbonate dry sliding trials. In each case a higher rate of friction force increase coincided with debris formation. No debris was produced in the ultra high molecular weight polyethylene dry sliding trials, and the friction force trace was flat. An SEM analysis of the polycarbonate and rigid PVC wear tracks revealed pitting consistent with the Delami-

nation Theory of wear. The effect of the lubricants was to significantly alter the form of the friction force traces, but not to eliminate wear in rigid PVC and polycarbonate.

The results of the investigation, particularly the delay in wear debris generation, indicated that a fatigue wear mechanism appeared to exist in dry metal pin-on-polymer disk sliding systems. A qualitative wear model was developed to relate the in-situ SEM observations and the results of the pin-on-disk trials.

ACKNOWLEDGEMENTS

The author gratefully acknowledges the patience and persistence of Dr. Norman S. Eiss, Jr., in directing this effort. His encouragement enabled me to complete the course requirements and to execute the research that resulted in this work. The author acknowledges Dr. David Dwight of the Graduate Committee for his guidance and recommendations on the SEM investigations. Dr. Michael Furey is acknowledged for his assistance in the lubrication aspects of this work, and of course for his agreement to become a member of the Committee after the departure of Dr. Custer.

I was able to complete this work only because of the love and understanding of my wife Deborah, whose "crisis management" was always appreciated but rarely recognized to the extent it should have been. And of course my daughter Ryland, whose smiling eyes always reminded me why this work needed to be completed.

CONTENTS

LIST OF FIGURES

Figure Page

LIST OF TABLES

INTRODUCTION

The primary direction of tribological research presently being conducted at Virginia Tech under the direction of Dr. Norman S. Eiss, Jr., is to characterize abrasive wear behavior of polymers as a function of mechanical properties and surface topography. Since 1975, surface topography measurements in conjunction with computer developments have been used to characterize wear surfaces. In addition, predictive wear models have been developed and verify that wear measurements made were found to agree within an order of magnitude of each other (1).

One of the earliest attempts to model abrasive wear came from the first phase of experimental work from 1974 to 1977 under a grant from the U. S. Army Research Office to study polymer wear by transferred films. Warren (2) observed the polymer transfer to ground steel surfaces, and using Orthogonal Cutting Theory (OCT), predicted a plane of maximum shear stress in the bulk polymer that would serve as a fracture plane during relative sliding. The fractured polymer would form wear debris. The position of the plane of maximum shear stress was designated the polymer shear angle. Warren observed wear debris in the Scanning Electron Microscope (SEM) and found that shear angles of polymers deposited on the surface under conditions of full penetration and single traversals could be measured. Warren

failed to observe the predicted shear angles and found little variation of shear angle with load. However, there was a significant variation of shear angles between polymers.

A subsequent model of abrasive wear was developed by Herold (3). This model incorporated the shear angle to predict wear particle volume. Herold assumed a two-dimensional wedge asperity model that penetrated an ideal rigid-plastic model polymer. The polymer flow pressure, P_m, was most important in determining the amount of penetration and was taken as three times the yield stress. Herold neglected strain rate dependency and strain hardening, interfacial components contributed by friction and tangential cutting forces, visco-elastic deformation, and material removal.

Herold's basic assumption was that the wear particle would be formed when the shear angle of the particular contacting polymer was less than the flank angle of the cutting side of the asperity as in Figure 1. He correctly observed that all asperities have continuously varying flank angles. The improvement over Warren's model which predicted that the material would be removed to a thickness of asperity penetration depth, was that the maximum wear was equal to the asperity encountered material. Figure 2 shows that a layer that encounters an asperity has some of the material removed from the bulk while the remainder passes over the

a=Asperity Flank Angle

b=Polymer Shear Angle

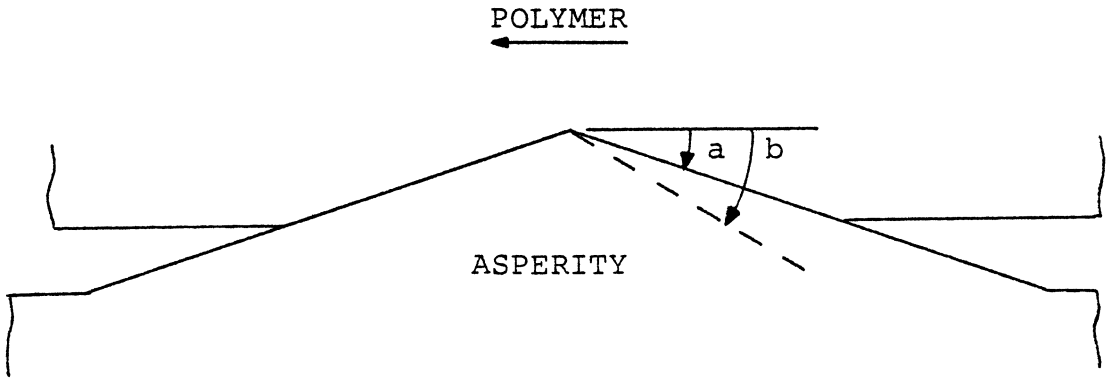

a) The asperity is not a cutter since a is less than b.

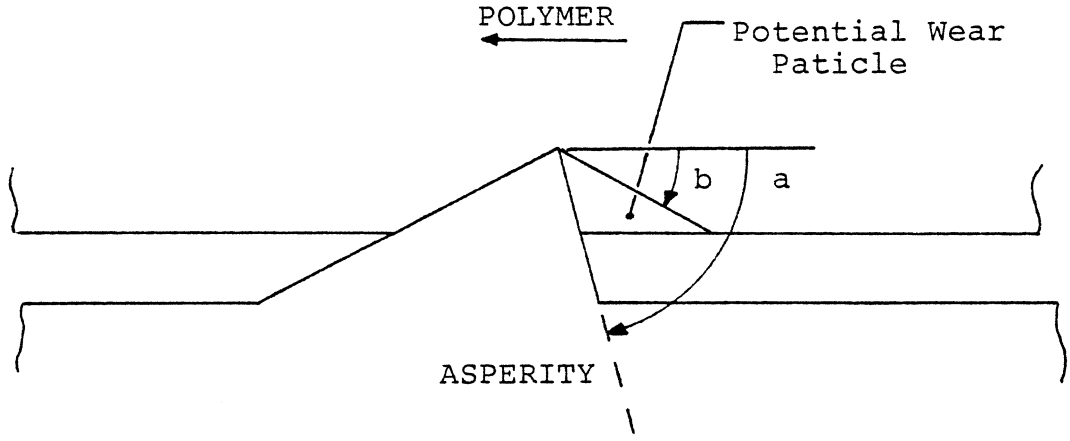

b) The asperity is a cutter since a is greater than b.

Figure 1. Asperity/Polymer interaction from Herold (3).

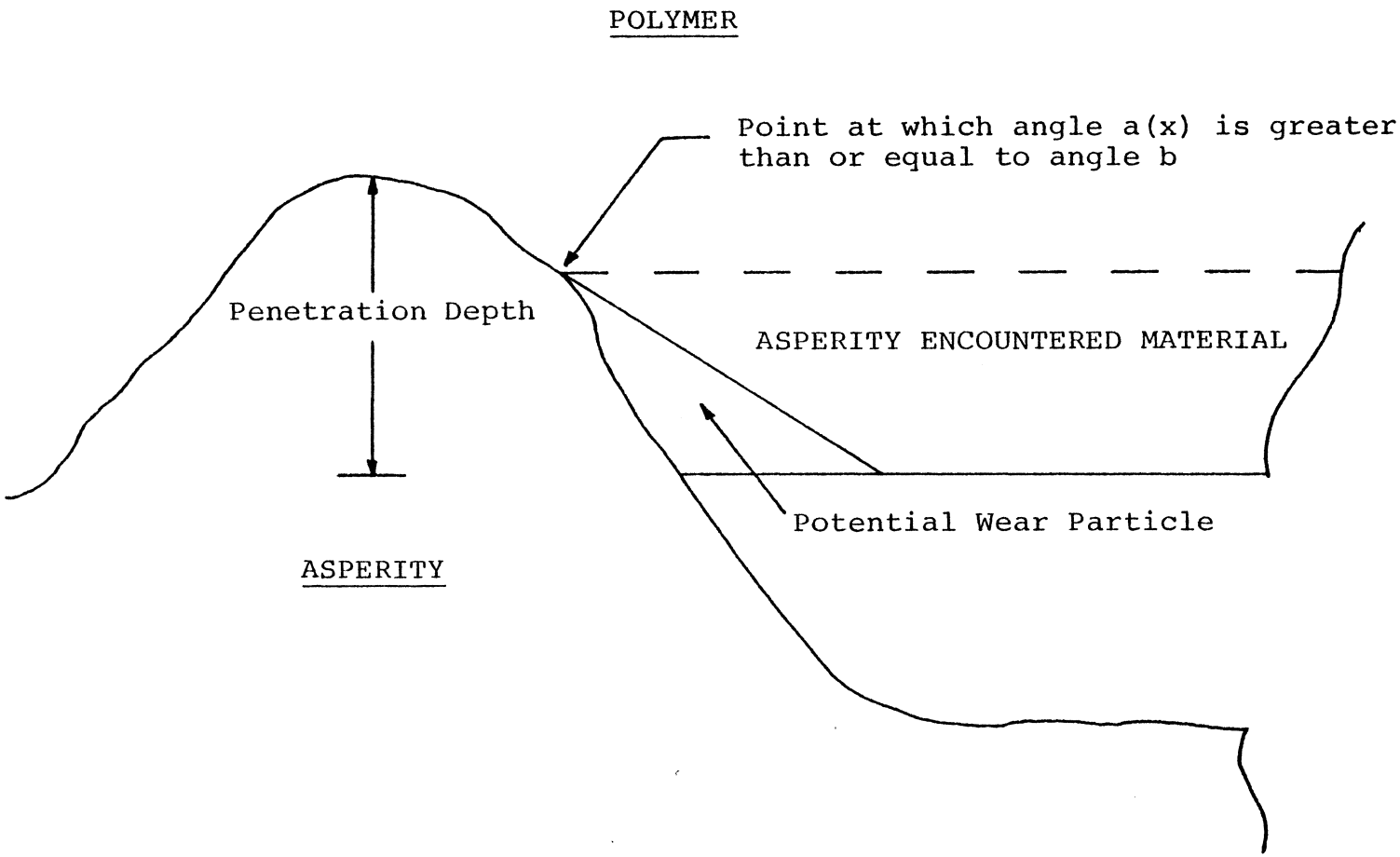

Figure 2. Illustration of asperity encountered material from Herold (3).

top in plastic and elastic deformation.

Herold constructed a deterministic surface consisting of many 25.4 μm thick stainless steel shims clamped together and bent to an appropriate angle to provide a 45 degree sawtooth surface. Six polymers were used to fabricate pins that were then traversed across the surface in a single pass. He observed the resulting wear debris in the SEM. For those polymers worn with a glass transition temperature (T_g) above room ambient, discrete uniform sized debris was observed which was similar to Herold's wedge model. For those polymers with T_g below room temperature, the polymer adhered to the asperity peaks and did not form discrete wear particles. Thus, Herold's model was limited to glassy polymers. Herold assumed that wear particles were formed as a function of sliding distance, and that the sliding distance term included an elongation-to-rupture term. Herold assumed that the debris was produced until the debris volume exceeded the void available between the asperity peaks. He neglected the possibility of load support by the polymer wear debris trapped in the void region, and any effects offered by debris transport and back transfer to the polymer pin. Although the model predicted that the wear rate would decrease for repeated sliding and that the wear rate would vary as a function of sliding direction and bearing area, it did not predict wear given a

polymer's mechanical properties, surface roughness, and normal loads applied.

Both Warren and Herold were only able to observe wear particles after sliding, thus the first area of experimentation conducted by the author was to develop the means through which close observations of debris production during abrasive wear could be made. To this end a testing stage was developed to rotate a polymer disk against spring-loaded steel counterfaces in the SEM. Direct observations of the abrasive wear process for rigid polyvinyl-chloride (PVC) and polycarbonate (PC) disks worn against several types of counterfaces were attempted.

Several attempts to directly observe wear particle formation in the SEM failed. Wear particles were produced in regions below the field of view. What was observed, however, was evidence of the plastic flow of the polymer around asperities, extrusion of debris from the counterface, the collection of debris particles into an aggregate which tended to separate the metal and polymer surfaces, and the cracking of the gold-palladium conductive coating. These results tended to support Herold's proposal that while some of the asperity encountered material would be removed, the remainder would pass over and around the asperity in elastic and plastic deformation. However, since no discrete particle formation was observed, Herold's assumption of particle

formation contingent on the shear angle of the polymer being less than the flank angle of the cutter could not be verified. A later multi-pass experiment in which a steel wedge was rotated against a static polymer surface showed that the wear particles were not produced immediately but occurred after several cycles of contact. The author concluded that the debris produced by abrasive wear during run-in could modify the asperity geometry and possibly the contact stresses. Further, this process could develop into a steady state wear regime where a fatigue mechanism could become an important mode of wear. This conclusion led to the development of a series of experiments to study surface fatigue in polymers.

Fatigue tests were conducted on the recently developed pin-on-disk wear machine. Provisions were made to reduce the abrasive mechanism by using a smooth steel ball bearing to penetrate a polymer disk, and altering the adhesive wear mechanism with simple lubricants. Experiments with rigid PVC, PC, and ultra high molecular weight polyethylene (UHMWPE) showed distinctly different friction traces. The lubricants modified the levels and configurations of the traces.

LITERATURE REVIEW

At the time of this investigation the theory of polymer fatigue was not well developed. A NASA literature review was conducted but few useful titles were found. Delamination Theory was considered the proper starting point for this review since it is closely allied with Fatigue Theory.

Adhesion and Delamination Theory

Tomlinson (4) was one of the first investigators to postulate metallic wear on an atomic basis. In his model surface atoms were removed by the action of attractive and repulsive forces at the interface. This model was improved by Archard (5) and Bowden and Tabor (6). Archard assumed that when contact occurred between two surfaces, the contact regions were small discrete areas that deformed plastically and formed metallic junctions. Wear was assumed to occur by removing fragments of metal from the surface. Breaking a junction in sliding provided a resistance component of friction. Most adhesive wear models including those for polymers follow the equation:

$$V = C \times \frac{W}{Pm} \times S$$

Where:

V = Wear Volume
W = Normal Load
Pm = Flow Pressure (3.0 x Yield Stress)
S = Sliding Distance
C = Constant

In Suh's Delamination Theory (7), the primary role of adhesion is to allow the transfer of forces across the interface. His theory improves upon simple adhesion theory by its inclusion of work required to create particles based on plastic flow and microstructure effects. Lubricants applied to the surface would tend to decrease the contact between the sliding members and thus reduce the tangential component of surface traction. Aside from decreasing adhesion, lubricants would distribute the normal load over a larger surface area. The wear rate would decrease as a result.

The basic mechanism of the Delamination Theory is shown in Figure 3. The theory proposes that the surface readily deforms during run-in. Dislocations that are present have a tendency to move out to the surface while others are driven into the bulk of the material. This action leaves a dislocation-depleted region below which cracks will form where the dislocations have been driven. On subsequent passes the cracks propagate parallel to the surface under the influence of a trailing tensile stress field and eventually terminate at the surface. The crack propagation to the surface forms a particle that is removed on later passes, leaving a pit.

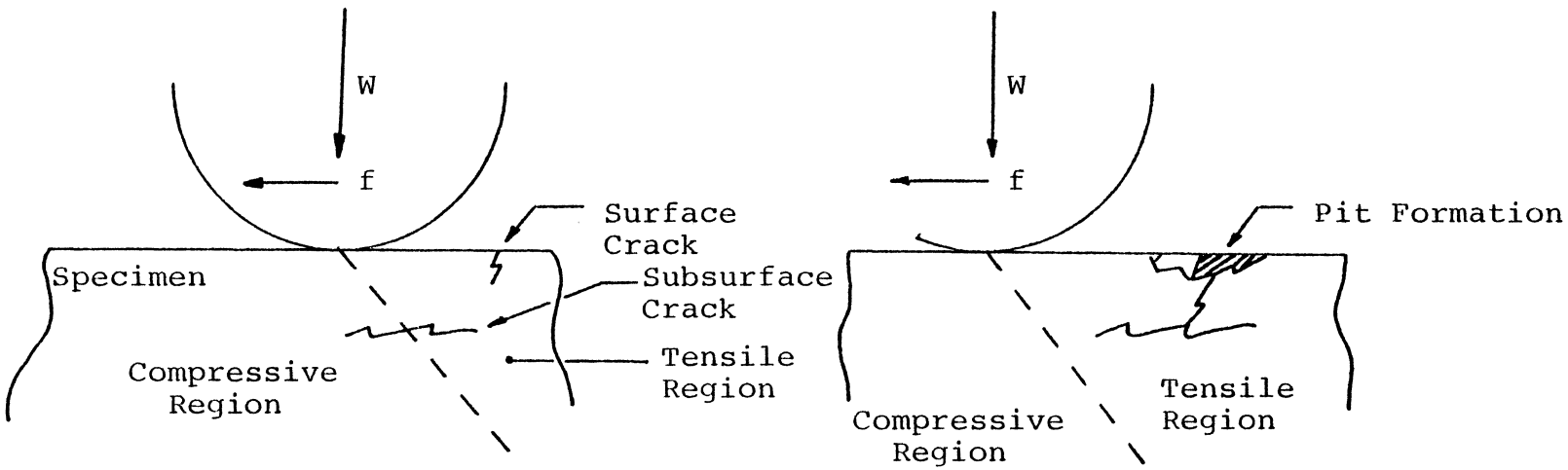

a) Passage of asperity forms subsurface cracks parallel with the surface.

b) Subsequent passes enlarge subsurface crack until it breaks out to form a pit.

Figure 3. Illustration of the Delamination Theory (7).

This theory is applicable to all materials in which subsurface crack nucleation and propagation mechanisms operate including thermoplastics with inclusions. On the other hand, glassy thermosetting plastics tend to fail through surface cracking and pure thermoplastics fail either by surface melting or continuous deformation.

Polymer Fatigue

The study of the fatigue properties of polymers has only recently developed in earnest. As in the wear of metals, fatigue is generally considered a mechanism of wear for polymers. The author found little published material in the area of surface fatigue, but several studies have been conducted that describe polymer performance in cyclic uniaxial and bending stress tests and relate the performance to fatigue wear.

Dowson et. al. (8), were the first to propose a surface fatigue wear mechanism in a unidirectional wear test. Using a tri-pin-on-disk machine, ultra high molecular weight polyethylene (UHMWPE) pins were loaded against a rotating steel disk. Two distinct periods of wear were noticed after a run-in period. The first period was characterized by a constant wear rate that coincided with the appearance of a transferred film. In the second period the wear rate increased. This increase was attributed to the presence of cracks on the pin, transverse to the direction of wear. It

was thought that these cracks were due to a fatigue mechanism. Dowson failed to elaborate on any possible mechanism or detail the effect of long term sliding on the established transfer film.

Crawford and Benham (9), reported that the application of a cyclic stress in the uniaxial test caused an acetal copolymer specimen to increase in temperature with the result that failure occurred by either an initial temperature rise and stabilization that allowed conventional crack initiation and propagation to occur, or that the temperature continued to rise until thermal softening occurred. Rabinowitz and Beardmore (10), reported on the cyclic stress-strain behavior of rigid polymers such as PC which showed a large decrease in the deformation resistance prior to crack formation. Amorphous polymers with moderate ductility such as polymethylmethacrylate (PMMA) showed a slight decrease in deformation with crazing playing a dominant role in decreasing fatigue resistance. Brittle polymers were essentially stable in cyclic deformation, but the fatigue resistance of these materials was sensitive to strain amplitude.

In an attempt to relate standard fatigue data with actual sliding conditions, Jain and Bahadur (11), derived a wear equation using the concept of fatigue failure due to asperity interactions. They considered polymer sliding on

metal as their experimental system. As in delamination, the trailing tensile field was considered responsible for crack initiation and propagation. The deformation in the contact area was considered elastic with the asperities modeled as spherical tips. The wear rate depended upon the fatigue properties of the polymer, normal load, friction, modulus of elasticity, asperity density and radius of curvature, and the distribution and standard deviation of asperity heights. The rather complicated equation was verified (12) using a polymer pin-on-disk machine. The tested polymers included PMMA, PVC, and high density polyethylene (HDPE). Experimental and estimated wear rates were in good agreement. However, it should be noted that the fatigue wear equation estimated steady state wear rates only and that the moderate temperature increases which occurred could have changed the adhesion characteristics of the interface. Despite these limitations, these experiments lend support to the concept that repetitive surface loading might be responsible for the formation of wear particles.

SEM OBSERVATIONS OF WEAR DEBRIS FORMATION

Equipment Development

An SEM testing stage was developed to observe low speed abrasive wear. This stage is shown in Figure 4. Polymer disks were fixed to a machined pin and held in place with a small nut. The pin was rotated through a bevel gear mechanism that was connected to a control knob outside the vacuum chamber by a shaft and universal joints. The direction and speed of rotation were adjusted by hand. Steel counterface models were spring loaded against the edge of the polymer disk.

Asperity Models

Several counterface surfaces were used in the SEM trials. They included a sawtooth surface, 1018 steel surfaces ground flat with smooth, rough, and double asperity topographies. The double asperity surfaces were produced by first polishing the counterface and then making a single scratch. Some counterfaces were machined to a wedge shape which was a large scale model for a single asperity.

A sawtooth counterface profile was developed following the general outline developed by Herold (13). The technique required to produce this profile proved to be difficult to master, particularly since a 6.4 mm square base was required to fit into the spring barrel. All of the sawtooth profiles produced were found to be completely inferior to Herold's,

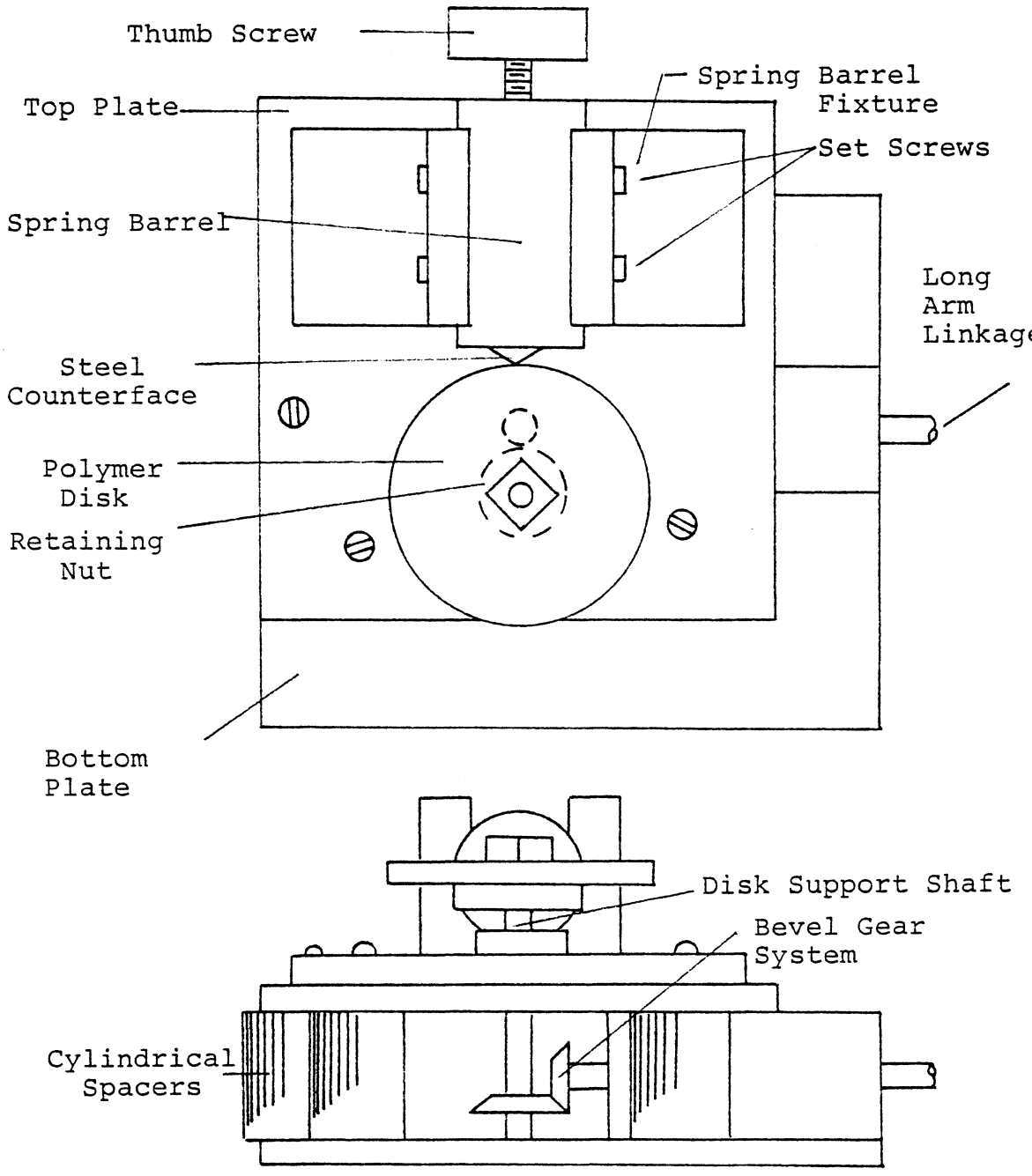

Figure 4. Testing stage for the SEM investigations.

and the one that was tested in the SEM was subject to gross deformation when loaded against the polymer disk. This approach was abandoned in favor of the steel blocks.

The ground 1018 steel counterfaces were found to be acceptable, particularly those with rougher surfaces that reduced the number of contacting asperities. This permitted the observation of a fewer number of regions where wear debris was produced. Typical peak-to-peak values were in the range of 13 to 15 microns. The counterface machined to the shape of a single wedge as shown in Figure 4 with sides at either 20 degrees or 40 degrees below horizontal was used to limit wear debris production to a single site.

Polymer Disks

Several plates of rigid PVC, PC, and UHMWPE were available from previous project experiments and utilized as disk materials in the SEM trials. The plates were first rough cut and then lathe turned to 27.9 mm diameter by 2.5 mm thick disks. The initial SEM observations showed that the disk edge blocked the view of the contact region. To circumvent this problem the disks were re-machined with a single 30 degree bevel, but were found to deform excessively when loaded against the counterface. To provide a stiffer edge new disks were machined with a double bevel, but these deformed under load also. Eventually, the best observations

were made by using the original disk configuration combined with the wedge counterface shimmed at a slight angle. This configuration is shown in Figure 5, and limited the contact to one region on the top of the edge of the disk. The field of view obtained in the SEM for this configuration is illustrated in Figure 6.

Before a disk was placed in the SEM testing state, it was sputtered with a thin gold-palladium conductive coating. Without this coating the non-conducting polymer would charge when bombarded with the electron beam. The effect of this charging was to cause the viewing area to brighten and become indistinct from other regions on the monitor. The coating itself is brittle in comparison to the underlying polymer, and would fracture into small particles during sliding.

Results

In the first tests, rigid PVC disks machined with a double bevel edge and carefully cleaned before coating were rotated against a rough steel counterface. Three observations were made:

1) plastic flow of the PVC,

2) polymer debris buildup and extrusion, and

3) load support provided by the debris aggregate.

Plastic flow is illustrated in Figure 7. The counterface asperity is the bulbous protrusion from the metal (dark)

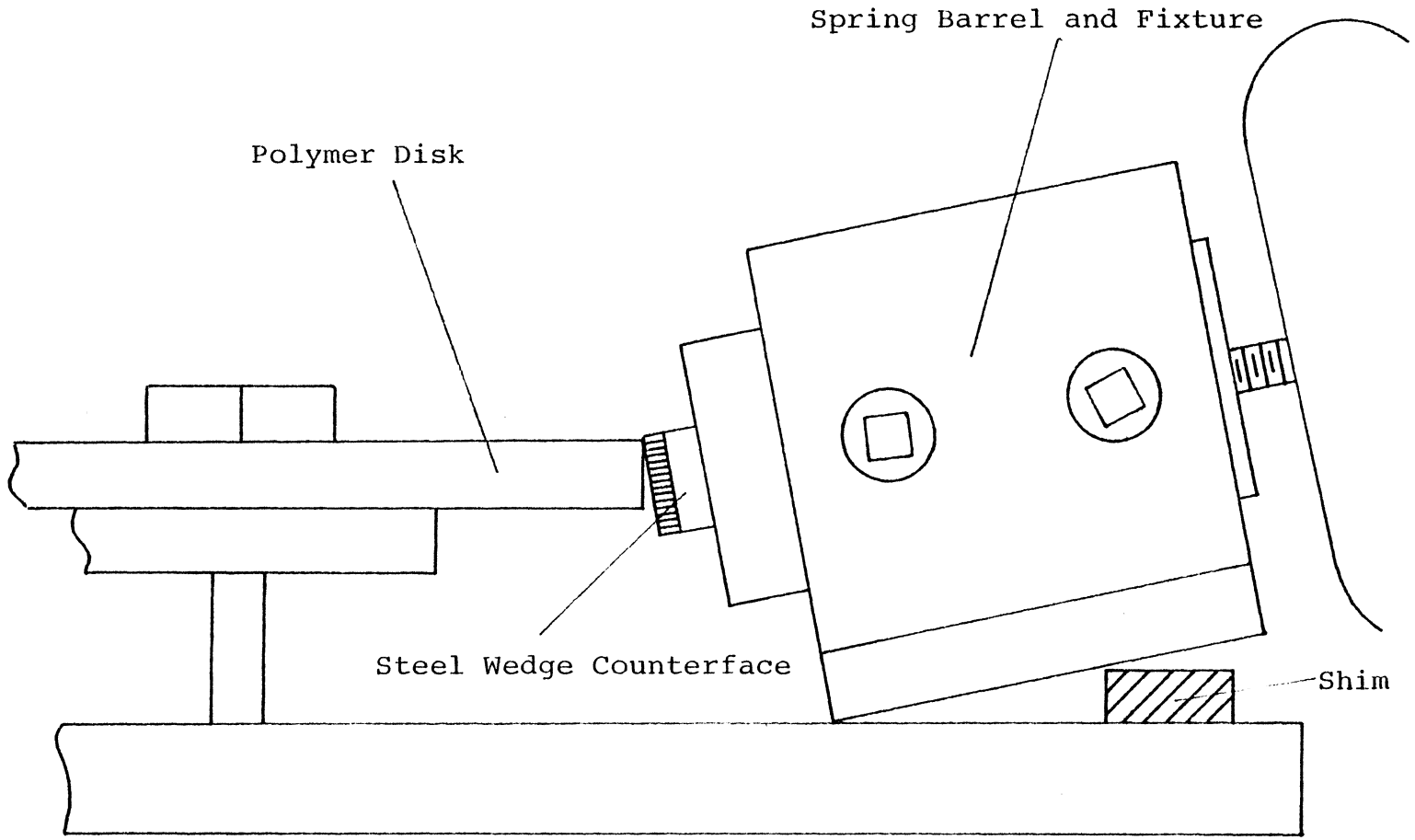

Figure 5. Polymer disk/shimmed counterface for best SEM viewing.

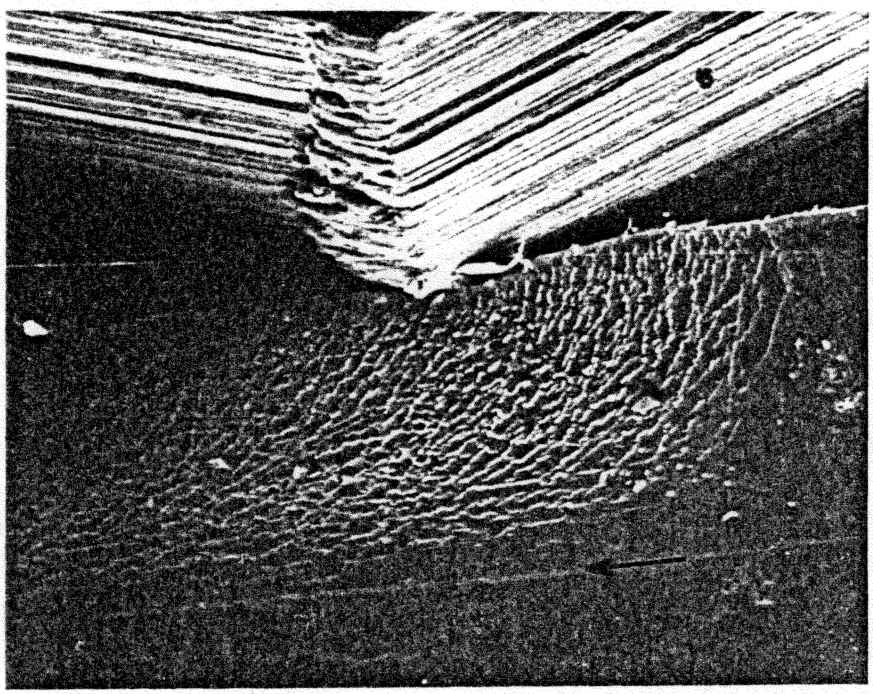

Figure 6. Typical field of view for the polymer disk and shimmed wedge counterface combination (PC-X285).

Figure 7. Evidence of plastic flow around the asperity during deformation (rigid PVC-X500).

half of the photo deforming the polymer. The plastic flow appeared as the curving dark streak, starting near the edge of the asperity and extending past at a constant distance from the edge of the disk. It was thought that the flow region resulted from permanent upward folding of the edge of the disk. However, a visual examination of the disk after the experiment showed no obvious lip on the disk edge.

Plastic deformation can lead to localized failure which results in debris production. The mechanism through which this failure would occur can be attributed to abrasive wear. However, the effects of plastic deformation on subsequent wear is speculative. Though strain hardening by cyclic loading leads to fatigue wear in metals, there is no evidence that this process occurs in polymers (14). Polymers have low thermal conductivity and high damping which contribute to a temperature rise during cyclic loading, and thus thermal softening could lead to failure without propagation of cracks. In addition, it has been proposed that cracks can be initiated and propagated by principal tensile stresses in sliding under conditions of elastic deformation (15).

With continued rotation, debris buildup occurred in the valley in front of the asperity. Since the experiment was confined to a single pass and the disk was cleaned carefully prior to coating, the debris was probably formed at the

asperity. The debris accumulated until the point was reached where the disk had actually been lifted from the counterface. This is shown in Figure 8, and it was noted that no obvious plastic flow was occurring at the time. At some later point in rotation the debris aggregate started to extrude from the valley in a direction perpendicular to that of sliding. This extrusion is shown in Figure 9, and was clearly composed of smaller debris. The surface of the extruded mass conformed to the topography of the metal surface.

The accumulation and extrusion of debris seemed to play an important role in the overall wear process in two regards. On one hand, the availability of debris increased the bearing area and reduced asperity penetration. Additionally, the debris aggregate could alter the effective geometry of the asperity and reduce wear during sliding as suggested by Herold's Model. In either case, or in combination, an obvious decrease in plastic deformation resulted from this phenomenon. Unfortunately, when the disk was reversed and the extrusion was pulled from the valley the process could not be repeated when normal rotation was reintroduced. The clearance between the disk and counterface was probably maintained by debris buildup supporting the normal load below the field of view.

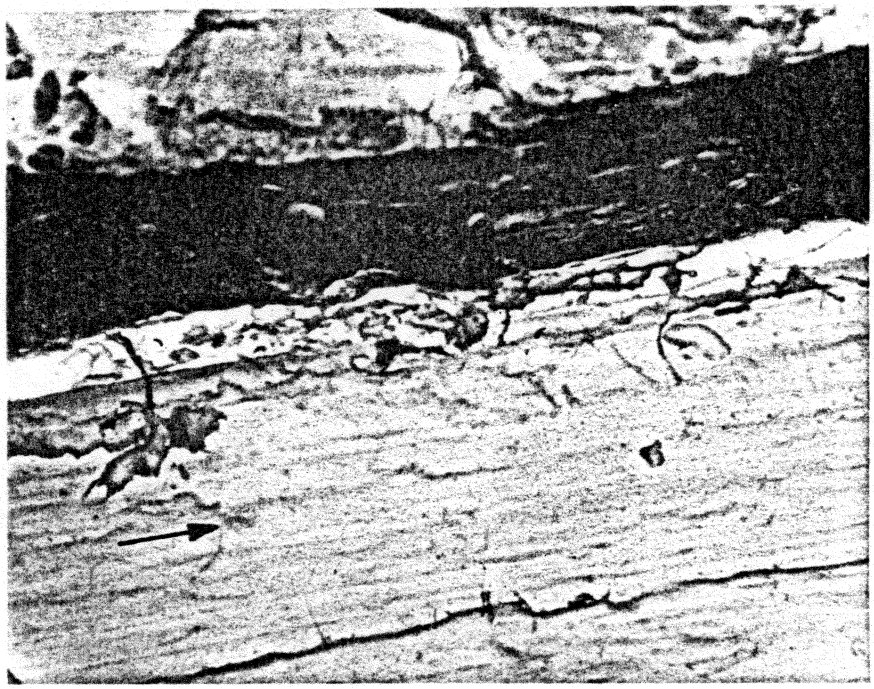

80 μm

Figure 8. Debris accumulation at the asperity resulting in load bearing and the separation of the disk from the counterface. No plastic flow was evident (rigid PVC-X250).

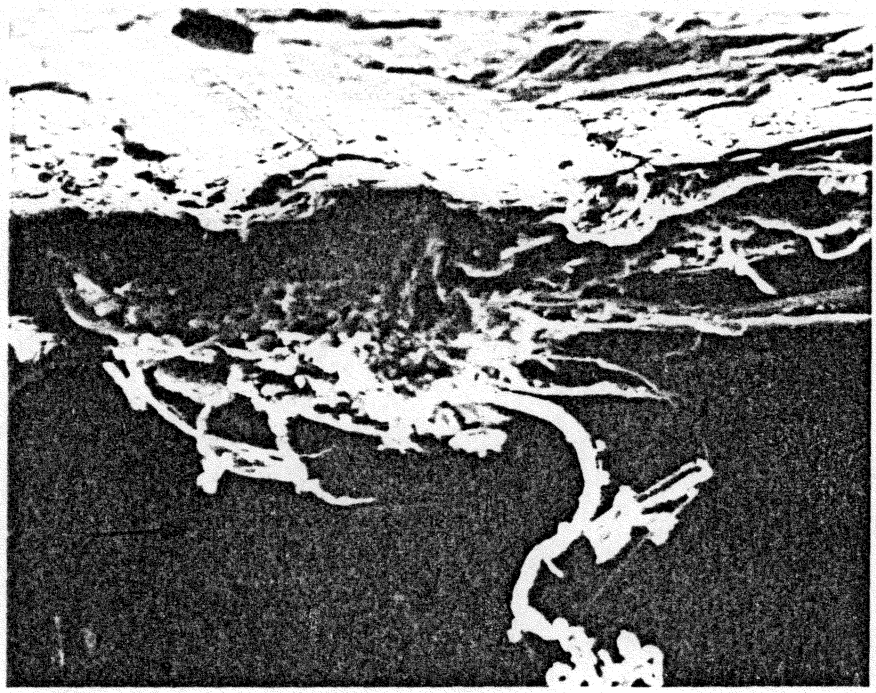

80μm

Figure 9. Extrusion of the debris aggregate from the asperity (rigid PVC-X250).

Further SEM sessions continued to show asperity modification due to debris buildup and extrusion. In sliding trials with rigid PVC and the double asperity counterface, debris were produced and extruded at both asperities as shown in Figure 10. The extrusions appear as a scalloped-like distribution of chunk debris, and are not dissimilar to the debris shown in Herold's PCTFE wear trials on the deterministic surface. Figure 11 shows that with continued sliding, debris aggregate caused plastic deformation at a point far removed from the asperity. This action may have effectively reduced the asperity flank angle and reduced wear, although as before the formation of particles could not be observed.

In trials with the steel wedge counterface, extreme deformation of the polymer around the asperity during rotation was noted. This deformation is shown in Figure 12. These trials also provided evidence of brittle microfracture of the conductive coating as seen in Figure 13. In this case the polymer was polycarbonate. A sequence of photographs in Figure 14 showed that bulk deformation, debris buildup, and aggregate extrusion occurred in wear of PC. Given the large volume of debris, it was not expected that conductive debris was the major constituent of the aggregate.

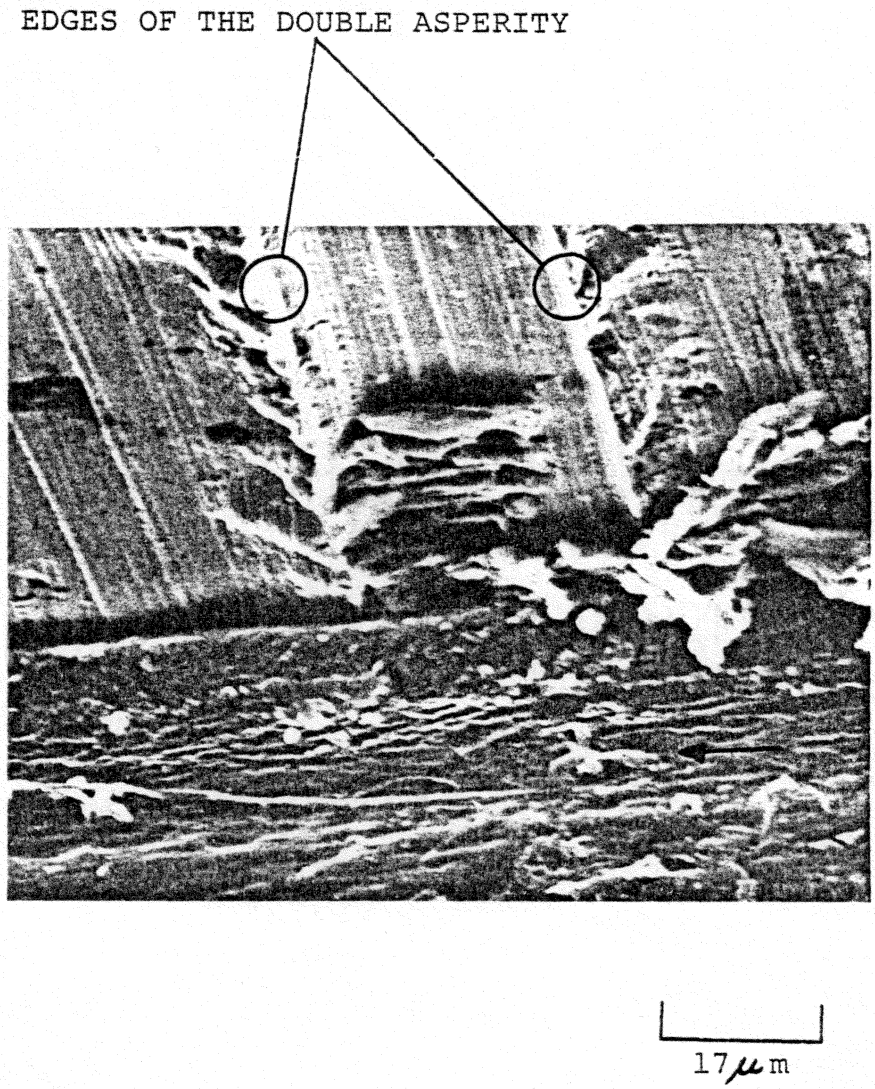

Figure 10. Debris buildup and extrusion from the double asperity counterface (rigid PVC-X1200).

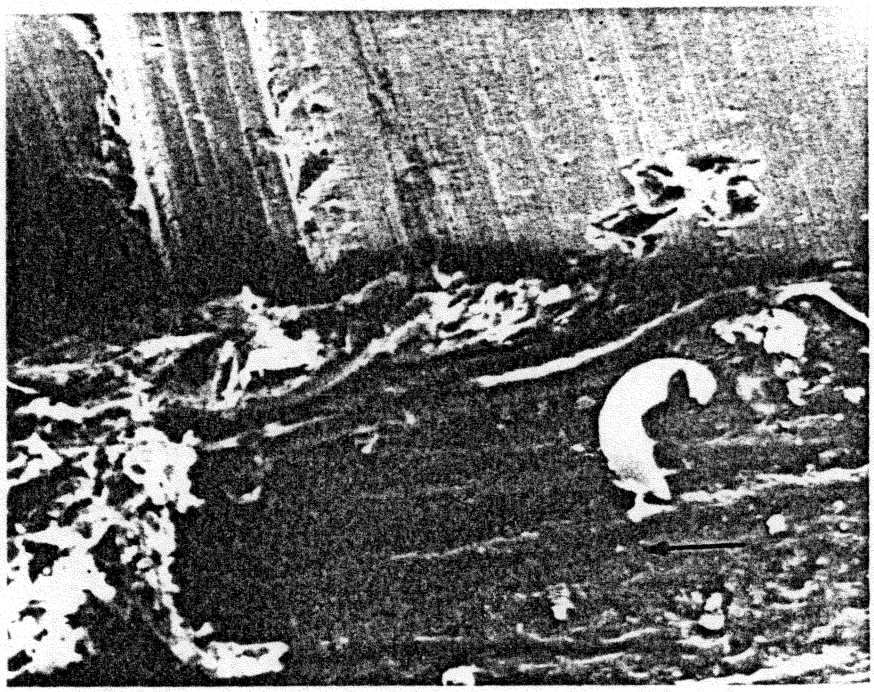

34 μm

Figure 11. Debris aggregate extrusion causing significant plastic deformation on the leading edge of the asperity (rigid PVC-X600).

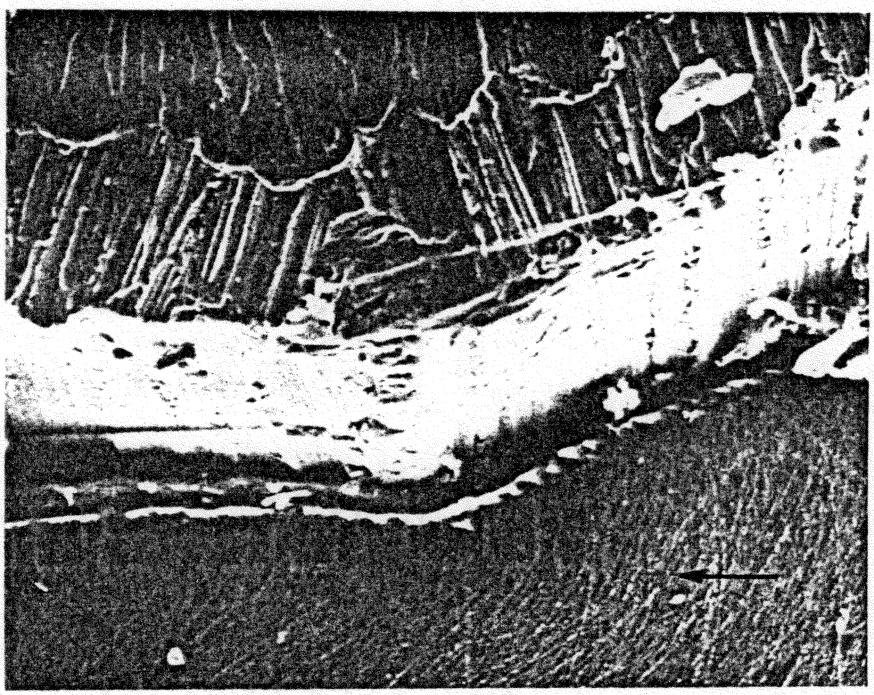

34 μm

Figure 12. Extreme deformation around the apex of the steel wedge (rigid PVC-X600).

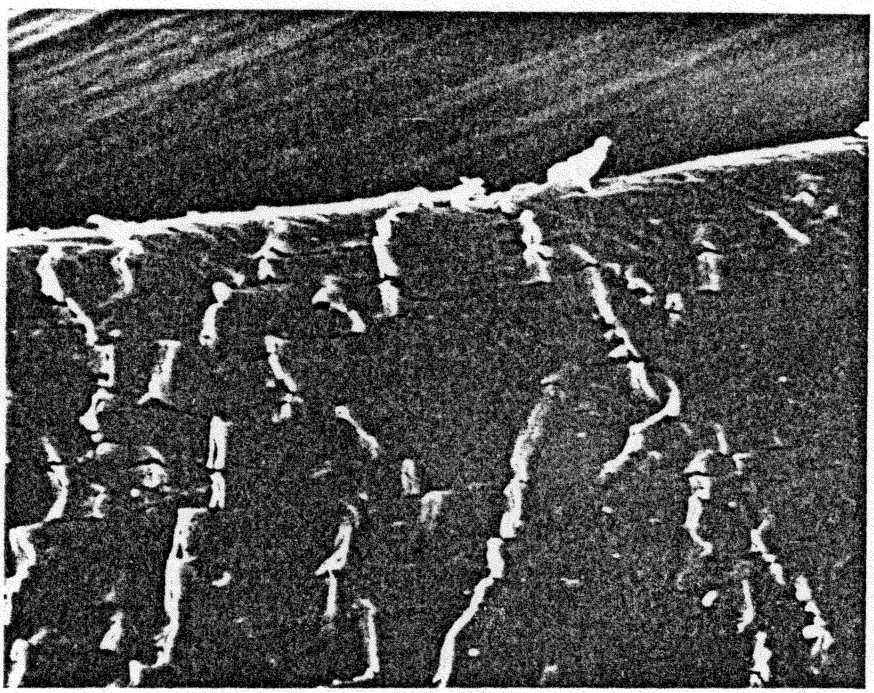

7 μm

Figure 13. Brittle microfracture of the gold-palladium conductant coating prior to contact with the asperity wedge (PC-X2850).

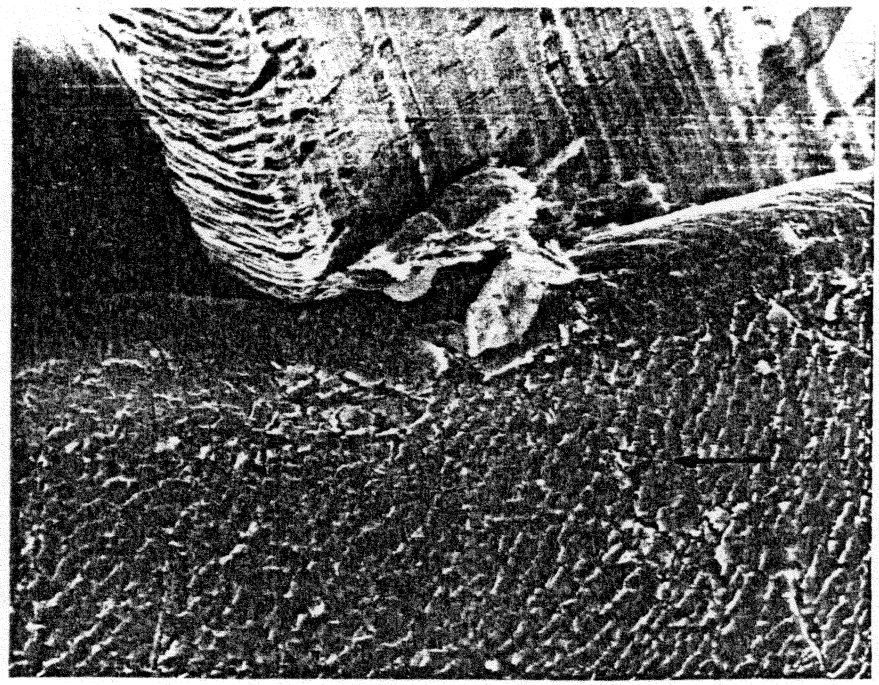

(a)

18 μm

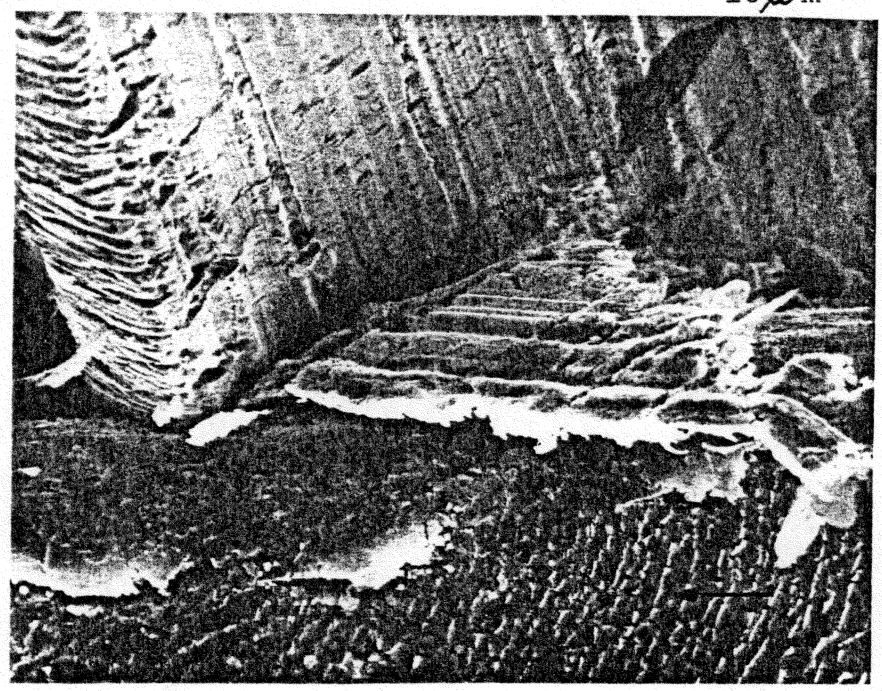

(b)

18 μm

Figure 14. Polycarbonate debris buildup (a) and extrusion (b) from the wedge asperity (PC-X1100).

Multiple passes and the corresponding cyclic effects on subsequent wear were not studied in the experiments described above. A simple trial was devised to investigate multiple pass sliding and to observe these effects in the SEM. Since the author had been unable to see the production of individual wear particles because of field of view limitations, and since multiple passes would remove the conductant coating and charge the underlying polymer, the polymer and metal surfaces were reversed. A small steel cam was machined with a wedge-shaped tip having an included angle of 90 degrees, drilled and tapped, and screwed onto the disk shaft. A rigid PVC plate was fixed to the spring barrel and the cam was rotated against its surface. SEM observations were taken from the apex of the cam after it had slid against the polymer and rotated an additional 180 degrees. It required several passes over the polymer surface before debris was produced. Examination of the polymer plate with a light microscope afterwards revealed a smooth wear surface marked by several large pits with apparently rough fracture surfaces. These observations were considered evidence that a delamination-type mechanism was occurring.

Discussion

The SEM experiments showed that as the polymer disk was rotated against a hard counterface, wear particles were formed or collected in the interface. The individual

particles formed a cohesive mass that altered the subsequent wear process by either supporting the load and/or modifying the effective asperity geometry to limit deformation and reduce its effectiveness as a cutter as proposed by Herold. Both rigid PVC and PC extruded from the leading valley of the contacting asperity in a direction perpendicular to sliding. It was not known why or when the aggregate began to extrude, though it is likely that the event is dependent on rate of valley filling, normal load, and friction between the debris and the surfaces.

It was concluded that the debris accumulation-extrusion process is a result of abrasive wear and that it can alter the geometry of an asperity, reduce abrasion, and perhaps result in a steady state wear condition. These observations and the literature suggest that a fatigue mechanism may be an important wear mode in the steady state regime. To this end the author was motivated to start a subsequent investigation into low-cycle surface fatigue.

FATIGUE WEAR EXPERIMENTS

The results of the SEM observations for single pass trials indicated that material buildup altered the asperity geometry and decreased the interfacial pressure which reduced abrasive wear. The multipass trials indicated that several passes or stress cycles were necessary before wear particles were produced. These observations indicated that, after an initial run in which the asperities became modified by transferred wear debris, the steady state wear may be one of fatigue. Since fatigue studies in the SEM would be too lengthy because of low cycle rates, pin-on-disk tests to study fatigue were initiated.

Apparatus and Calibration

The pin-on-disk wear machine used in these experiments is shown in Figure 15. The trials associated with this work were the first studies done using this machine. The normal load was introduced by a piston arrangement connected to a regulated nitrogen supply. The normal load was directly proportional to the nitrogen pressure. This loading arrangement had a low mass and thus limited the dynamic loading problems associated with using a dead weight to apply the normal load. The pin displacement was sensed by a proximity detector that measured the relative position of a metal cantilever on the piston shaft. Friction force was obtained through a cantilever beam displacement measured by

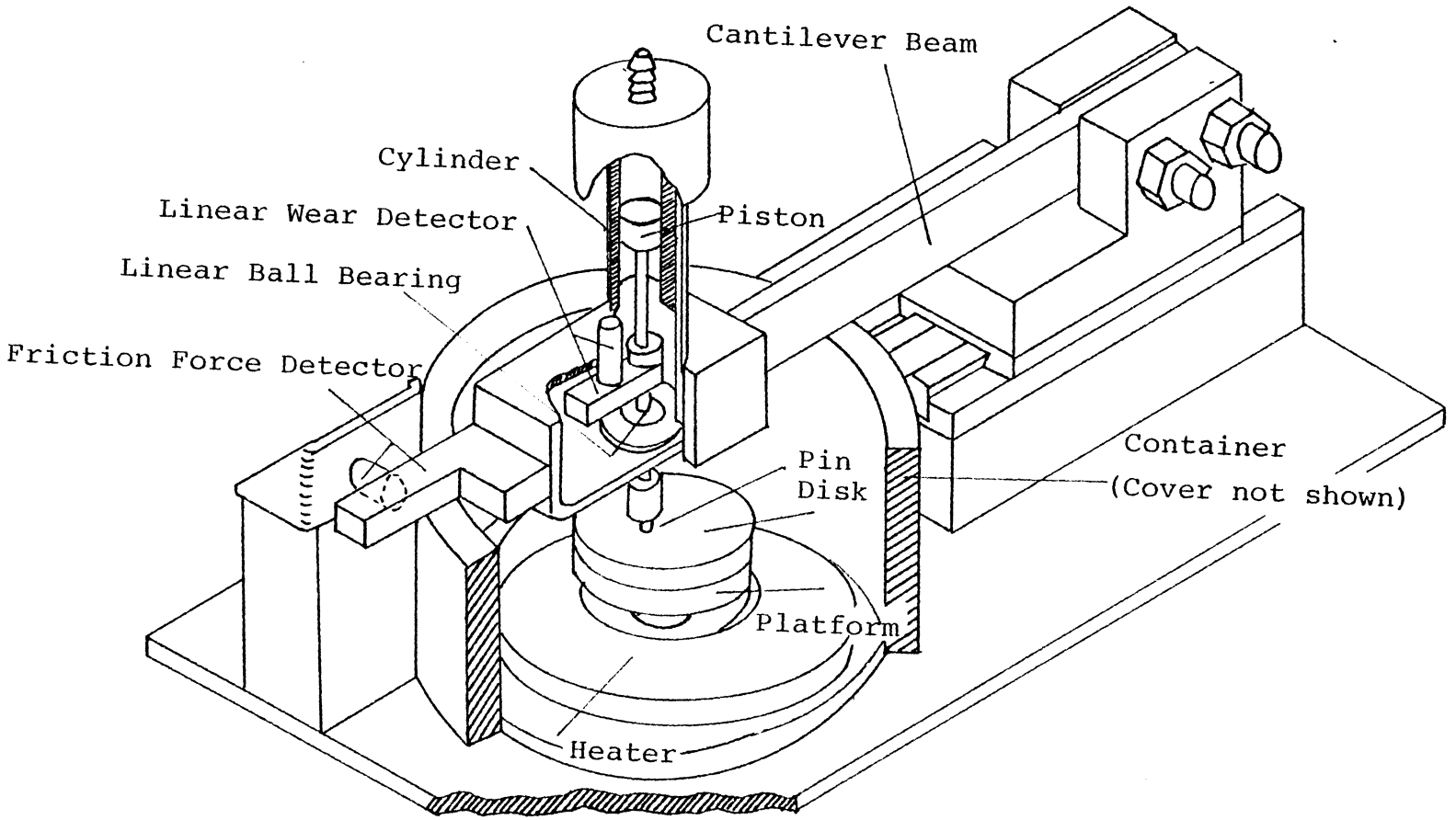

Figure 15. Pin-on disk wear machine (1).

a second proximity detector. Both the pin displacement and friction signals were recorded on separate X-Y plotters.

The cantilever system that provided the friction force deflection was calibrated before the experiment started. At a specific voltage level and recorder range, graduated weights were hung from a wire connected to a pin. The wire was placed over a pulley so that the tangential pull perpendicular to the direction of normal load produced an artificial friction force. At each incremental weight, the Y-axis displacement of the X-Y Plotter was marked. The process was repeated for specific distances from the centerline of the spindle corresponding to preselected radial distances. As a result, the friction force measured during individual trials at identical radial distances could be related to one another. The pin displacement was calibrated after the conclusion of each run by placing a 0.00254 cm stainless steel shim under the loaded pin, withdrawing it, and recording the trace deflection on the X-Y plotter.

Abrasion and Adhesion Effects

The pin was a 0.318 cm diameter alloy steel ball bearing glued into an aluminum socket. The socket was slipped onto the piston shaft and fixed in place with a set screw. The ball bearing was considered the invariant component of the sliding system. The surface roughnesses of both pin and disk were considered negligible, though no

provisions were taken to polish the as-received surfaces. The formation of wear particles was assumed to be initiated from the polymer disk and were not considered viable agents for third-body abrasion by virtue of their relative softness. The surface attraction in a metal/polymer sliding system is limited to weak Van der Waals bonds, and thus reduced the likelihood of adhesive wear. Further, temperature effects such as thermal softening were neglected since loading was small and the sliding speed of 4.0 cm/s was slow.

Test Polymers

The polymers tested were PC, UHMWPE, and two types of rigid PVC with different molecular weights. These polymers offered a broad range of structure and mechanical properties. PC are high molecular weight, low crystalline thermoplastics characterized by toughness, transparency, and dimensional stability. PC is effected little by humidity, and is generally unaffected by grease, oils, and acids. The resins are soluble in chlorinated hydrocarbons and are attacked by aromatic solvents, esters, and ketones which cause crazing and cracking in stressed parts (16). Rigid PVC is a hard, tough semi-crystalline thermoplastic that can be compounded to offer a wide range of properties. The base resin is soluble to aromatic solvents, ketones, aldehydes, napthalenes and some chloride, acetate, and acrylate esters (17). UHMWPE is a highly

crystalline thermoplastic, and is characterized by good abrasion resistance and a low coefficient of friction. Chemical resistance is excellent (18). Of the polymers described above, only UHMWPE is used as a bearing material in engineering applications. Properties of each polymer are listed in Table 1.

The specimens were 4.4 cm by 4.4 cm by 0.3 cm thick plates. A center hole was drilled into each plate and the plate threaded onto the spindle and held by a nut. The plate was fully supported by the spindle and the wear tracks were entirely contained on the spindle platform to minimize deflections.

To determine whether the steel pin loaded against the polymer plate caused the polymer to be plastically deformed prior to sliding, Hertzian (elastic) theory was employed. The appropriate Hertz equation for a sphere on a plate only applies to static loading in the elastic regime. The maximum shear produced by elastic loading occurs at some point below the contacting surface and may be responsible for surface fatigue failure by originating and propagating cracks in this region (22). The introduction of a tangential surface load through friction inreases the principal stresses at the surface (23), and tends to lower the loads required for plastic deformation. Using Hertzian analysis the maximum pressure at the interface can be calculated. If this

TABLE 1

MECHANICAL PROPERTIES OF TESTED POLYMERS

Properties	PC[a]	PVC I[b]	PVC II[b]	UHMWPE[a]
Tensile at Break (MPa)	65.5	52.8	39.6	38.6
Tensile Yield (MPa)	62.0	60.4	60.9	24.5
Elongation to Break (%)	110	66	31	453-525
Tensile Modulus (GPa)	2.38	3.84	3.88	1.10[c]
Molecular Weight	-	70000	40000	-

[a]Ref. (19)

[b]Ref. (20)

[c]Ref. (21)

pressure is greater than the yield stress of the polymer, then the polymer is plastically deformed. The governing equations and calculated results for the applied normal loads of 10.0, 8.5, and 7.2 N are shown in Table 2. In each material/load combination the polymer was plastically deformed.

Lubricants

A series of trials were conducted using a lubricant between the steel pin and polymer plate. The trials were run under the same loading and speed conditions as in dry sliding for each polymer noted in the previous section. The lubricants, their room temperature viscosity values, and a subjective rating of their wettability taken at the time of the trials are listed in Table 3. Each polymer tested was chemically resistant to each of the lubricants.

Given the parameters of the trials, it was necessary to calculate the lubrication film thickness to determine whether the presence of the lubricant interfered with polymer-metal contact. The Kirk-Archard (24) equation for elastrohydrodynamic lubrication (EHL) was used to calculate the film thickness of mineral oil to be between 3.6-3.9 E-8 m for each polymer/normal load combination. This value is near the bottom end of the generally accepted thickness range attributed to EHL theory, and may have extended into the "mixed" lubrication regime (25). This conclusion is

TABLE 2

DETERMINATION OF PLASTIC STATE FOR POLYMERS

Polymer	W(N)	a(m)	Pressure(MPa)	YS(MPa)	State
PC	10.0	1.62 E-4	121.3	62.0	Plas.
"	8.5	1.54 "	114.1	"	"
"	7.2	1.45 "	109.0	"	"
PVC I	10.0	1.39 E-4	164.7	60.4	Plas.
"	8.5	1.31 "	157.7	"	"
"	7.2	1.24 "	149.1	"	"
PVC II	10.0	1.38 E-4	167.1	60.9	Plas.
"	8.5	1.31 "	157.7	"	"
"	7.2	1.24 "	149.1	"	"
UHMWPE	10.0	2.09 E-4	72.9	24.5	Plas.
"	8.5	1.98 "	69.0	"	"
"	7.2	1.88 "	64.8	"	"

a(m) = Radius of the Contact Area

$$= \left[\frac{3 \times W}{8} \times \frac{((1-\nu_1^2)/E_1) + ((1-\nu_2^2)/E_2)}{(1/d_1)+(1/d_2)} \right]^{1/3}$$

Where: W = Normal Load

ν_1 = Poisson's Ratio for Polymer (0.40)

ν_2 = " " " Steel (0.292)

E_1 = Elastic Modulus for Polymer

E_2 = " " " Steel (207GPa)

d_1 = Diameter of Plate (Infinite)

d_2 = " of Steel Ball (0.00317 m)

Pressure = $W/\pi a^2$

TABLE 3

LUBRICANT TYPES/VISCOSITY/WETTABILITY

Lubricant	Viscosity (N s/m^2)	Wettability		
		PC	PVC II	UHMWPE
H_2O	0.00089	Fair	Poor	Poor
H_2O + TSP[a]	0.00089	Good	Good	Poor
Methanol	0.00056	Good	Fair	Fair
Mineral Oil	0.700	Excel.	Excel.	Excel.

[a] 3% "Spic and Span" by mass. Cleaning agent is Trisodium Phosphate. Contains surfactant to improve wettability.

speculative since the surface roughness of the polymer was not available. "Mixed" lubrication occurs if the ratio of the film thickness and composite RMS roughness is less than one. The possibility of thin film lubrication was not considered for the other lubricants based on their much lower viscosities, but it was considered likely that their presence would interfere with adhesion bonding at the contacting areas. Based on the EHL calculation it was expected that some difference would be found between the mineral oil trials and trials with other lubricants.

A further lubrication effect that had been proposed by several authors was that of lubricants in surface cracks under normal load. When a lubricant has been "trapped" in a surface crack, under load it might act as a wedge against the crack root and propagate the crack further. On subsequent cycles this action could actually accelerate the rate of wear. Whether this action would be observed and quantified was unknown prior to the pin-on-disk trials.

Procedure

This work was divided into two phases of testing. Phase I was dry sliding trials for all polymers to determine if a fatigue mechanism existed. Phase II was lubricated trials run under the same conditions as in Phase I, for the purpose of studying the effect of lubrication on friction and pin displacement, as well as topography of the wear

track.

Before each trial the polymer plates were washed with methanol, wiped clean with a paper cloth, air dried, and stored in a cabinet to reduce surface contamination until tested. The appropriate identification number was scribed onto the plate. The metal pin was cleaned with a methanol soaked cloth and left to air dry. The pin position was adjusted to the proper radii (generally in the 1.78-2.03 cm range by 0.0635 cm increments). The rotational speed was adjusted at each radii so that the sliding speed was always 4.0 cm/s in each track. The load was applied by opening the nitrogen valve and adjusting the regulator to furnish either a 10.0, 8.5, or 7.2N normal load appropriate to the individual run. Both X-Y Plotters were zeroed and the voltage, range, and sensitivity levels checked. In Phase II, the lubricant was carefully introduced onto the plate so that it covered the surface without seeping over the sides. The plate and pin were not fully immersed, but rather surface tension kept the lubricant covering all wear areas.

After a final system check, the pin was lifted from the plate and the motor was turned on. Once the speed was checked the pin was lowered onto the plate. Immediately both X-Y Plotters were activated and a stopwatch started. The delay in performing this function was at most 3-5 seconds from the point when the pin was lowered. The

friction and pin displacement traces were continually monitored during the trial. The voltage level of the position transducers were checked for drift, and any changes were noted on the traces. For the longer duration lubrication trials more lubricant was added as needed to compensate for evaporation.

In Phases I and II, each trial was terminated two or three minutes after the friction level appeared to level off. Included in Phase I were additional trials which were terminated at specific revolutions or times to show the progression of wear track changes for SEM analysis.

The pin was wiped clean each time a new radius was used. The same pin was used for all tests. After the end of each trial the polymer plate was removed and cleaned thoroughly with methanol to remove contaminants and lubricants. It should be noted that each plate was cleaned to allow conductant to be sputtered onto the surface for SEM observations. It was an accepted fact that this practice would tend to eliminate evidence of debris disposition that might have been useful in identifying some aspects of the wear mechanism.

FATIGUE WEAR RESULTS

Phase I - Dry Sliding

Wear debris was produced in the rigid PVC and PC trials. In the rigid PVC case, the debris was not evident until the polymer disk had undergone several minutes of sliding. The debris was seen to adhere to the leading edge of the pin in an aggregate composed of smaller debris. The aggregate formation was preceded by the development of a visible track along the radius of sliding contact, which until this point had been indistinguishable from other non-sliding areas. A similar situation was observed in the PC trial in which debris was not produced immediately but after several loading cycles. The production of debris occurred in a much shorter period of time for PC than rigid PVC. No debris was produced in the UHMWPE trial. The following sections detail the results of the dry sliding trials. All actual friction force traces are contained in Appendix A.

Rigid PVC I and II

Friction traces for the two PVC I and three PVC II trials are shown in Figures 1-5A in Appendix A. Each trace, regardless of normal load, exhibited some form of a transition from a lower to a higher level of friction force. There was a high degree of variability between the number of cycles before the transition, the number of cycles during the transition, and friction levels. In some cases,

particularly at lower normal loads, it was difficult to identify a time at which the transition started since the friction increased gradually rather than sharply as illustrated in Figure 2A. In these cases the transition to an event was taken at the point where the curve slope changed.

In general, the higher friction forces were associated with those runs of a higher normal load. Often the final level was the same for each of the two 10.0 N normal load runs. For the 10 N runs in the rigid PVC II tests the friction trace decayed rapidly to a lower level immediately after the transition was completed. This is illustrated in the A and B friction traces around the 15 to 20 minute mark in Figures 1-3A. This phenomenon did not occur for similar PVC I trials, nor for runs conducted at 8.5 and 7.2 N normal loads in general.

Since the individual friction traces for PVC I and II varied widely, three specific points (or events) were chosen for a comparison of normal load and polymer composition effects on friction forces and sliding distance. These points were the beginning of the trace and the events corresponding with the start and end of the transition region. The time to an event as shown in the figures was converted to sliding distance in meters and the number of cycles. This data is contained in Tables 4 to 6.

Data from these tables clearly show three distinct regions corresponding to the rate of friction force

TABLE 4

BEGINNING FRICTION LEVELS FOR DRY SLIDING TRIALS

Polymer	No. of Data Points	Load (N)	Friction Force (N)	Coefficient
PVC I	4	10.0	.90 (.35)[a]	.09
"	2	8.5	.78 (.36)	.09
"	2	7.2	.74 (.30)	.10
PVC II	6	10.0	.93 (.34)	.09
"	3	8.5	.85 (.29)	.10
"	3	7.2	.65 (.26)	.09
PC	3	10.0	3.30 (.40)	.33
"	1	7.2	2.30 -	.32
UHMWPE	2	10.0	1.30 (0)	.13
"	1	8.5	1.36 -	.16
"	1	7.2	.57 -	.08

[a] Standard Deviation

TABLE 5

EVENTS AT THE BEGINNING OF TRANSITION FOR PHASE I

Polymer	No. of Data Points	Load (N)	Friction Force (N)	Cycles	Sliding Distance (m)	Coefficient
PVC I	4	10.0	1.45 (.41)[a]	119 (22)[b]	15.0	.15
"	2	8.5	1.26 (.37)	155 (50)	18.6	.15
"	2	7.2	1.19 (.33)	171 (51)	19.8	.17
PVC II	6	10.0	1.47 (.27)	230 (70)	28.9	.15
"	3	8.5	1.27 (.37)	191 (86)	22.9	.15
"	3	7.2	1.21 (.27)	187 (110)	21.6	.17

[a] Standard Deviation

[b] Standard Deviation Rounded to Nearest Whole Cycle

TABLE 6

EVENTS AT THE END OF TRANSITION FOR PHASE I

Polymer	No. of Data Points	Load (N)	Friction Force (N)	Cycles	Sliding Distance (m)	Coefficient
PVC I	4	10.0	2.93 (.39)[a]	250 (47)[b]	31.4	.29
"	2	8.5	2.55 (.52)	321 (21)	38.4	.30
"	2	7.2	2.20 (.25)	343 (132)	38.5	.31
PVC II	6	10.0	2.98 (.15)	306 (69)	35.9	.30
"	3	8.5	2.48 (.11)	300 (56)	35.9	.29
"	3	7.2	2.05 (.16)	347 (49)	40.2	.29
PC	3	10.0	4.80 (.10)	23 (11)	3.1	.48
"	1	7.2	3.67 -	60 -	7.2	.51

[a]Standard Deviation

[b]Standard Deviation Rounded to Nearest Whole Cycle

increase per unit sliding distance. The first region, Region I, was characterized by a continuous increase in the friction force level until a point was reached where the rate of change increased. From the friction traces it should be noted that the trace was not actually linear, but was often characterized by a higher rate of friction force increase within the first few minutes of the run. Although this part of the curve could be referred to as "run-in", the author makes no distinction at this point between this trace characteristic and the fact that the friction force often increased at a nearly constant rate thereafter through the remainder of the region.

The second, or Transition Region, was characterized by the highest friction force increase per unit sliding distance, and these rates were higher for larger normal loads. The PVC I transition occurred at a shorter sliding distance than that for PVC II, although the friction force levels were generally the same. The friction force at transition was always larger for higher normal loads. In rigid PVC I the transition region started at a shorter sliding distance at higher loads. The same observations could be made for the end of transition. As in Region I, the individual curves were generally not linear. The transition region was completed at the point where the friction force leveled off or started to drop abruptly.

In a careful examination of trial PVCT I4A, the sudden peak in the friction level at the end of transition (Track A), coincided with debris formation. For tracks C and D the friction was near the end of a "smooth" transition when debris was observed. Although the debris production was most carefully monitored in this particular trial, the phenomenon was common for the other rigid PVC trials as well. Often the debris formation was marked by an audible vibration from the piston shaft. This vibrating probably resulted from stick-slip between the ball bearing and the polymer surface.

The PVC II trials were terminated at the point where the friction force leveled off after transition. The PVC I trials were continued after the transition and defined Region III which was characterized by a generally stable friction level until the trial was terminated.

Pin displacement traces were taken during all the trials except PVCO 15A. The maximum depth of penetration from the traces was in the .0075-0.0076 mm range. Examples from three trials are shown in Figures 16 a-c. When a pin displacement trace was compared to its corresponding friction trace, few consistent and direct correlations between specific events were noted. However, most of the traces showed progressive penetration in Region I followed by a decrease in penetration somewhere in the Transition Region.

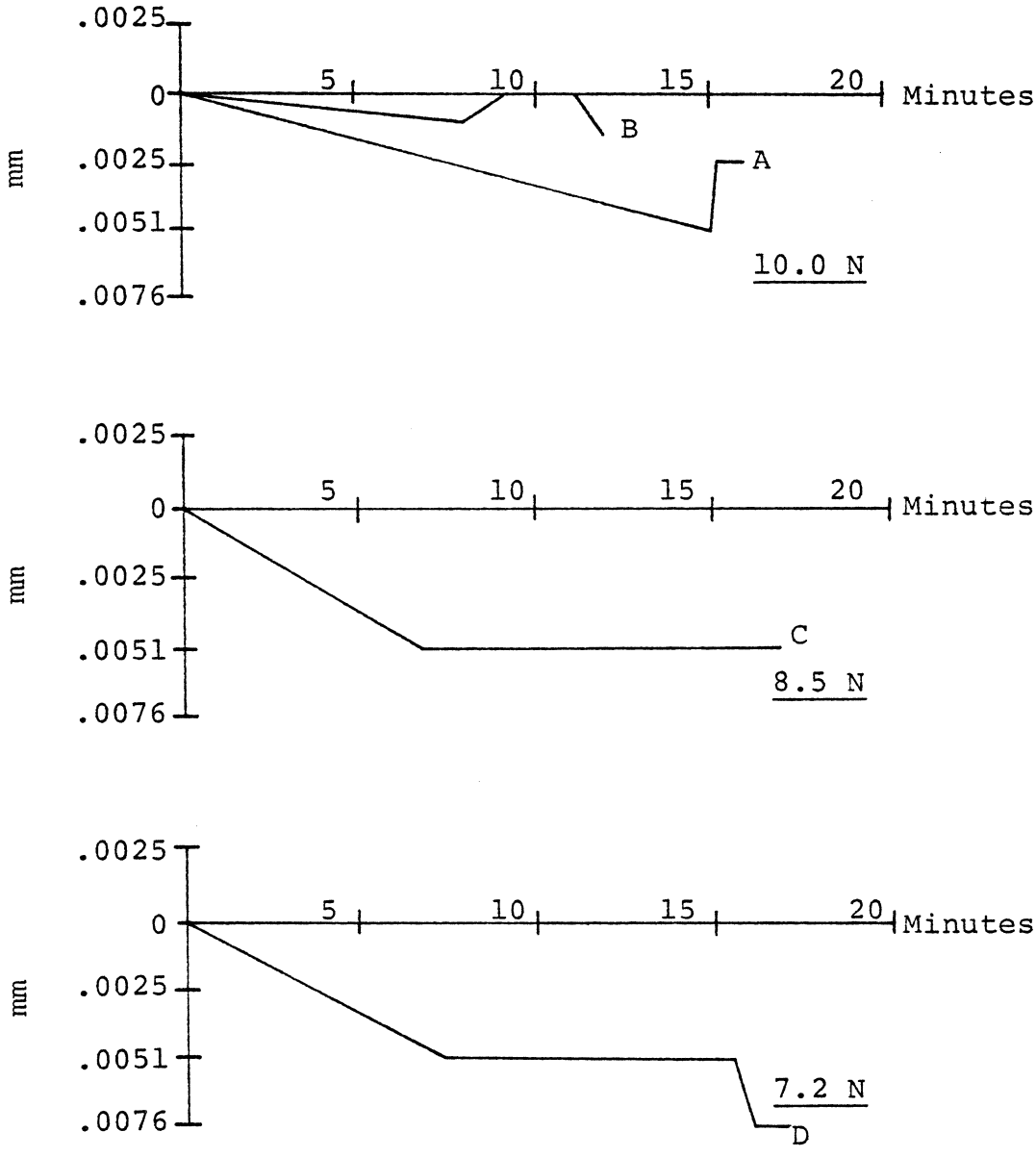

Figure 16a. Pin displacement trace for PVCT I4A in dry sliding (rigid PVC II).

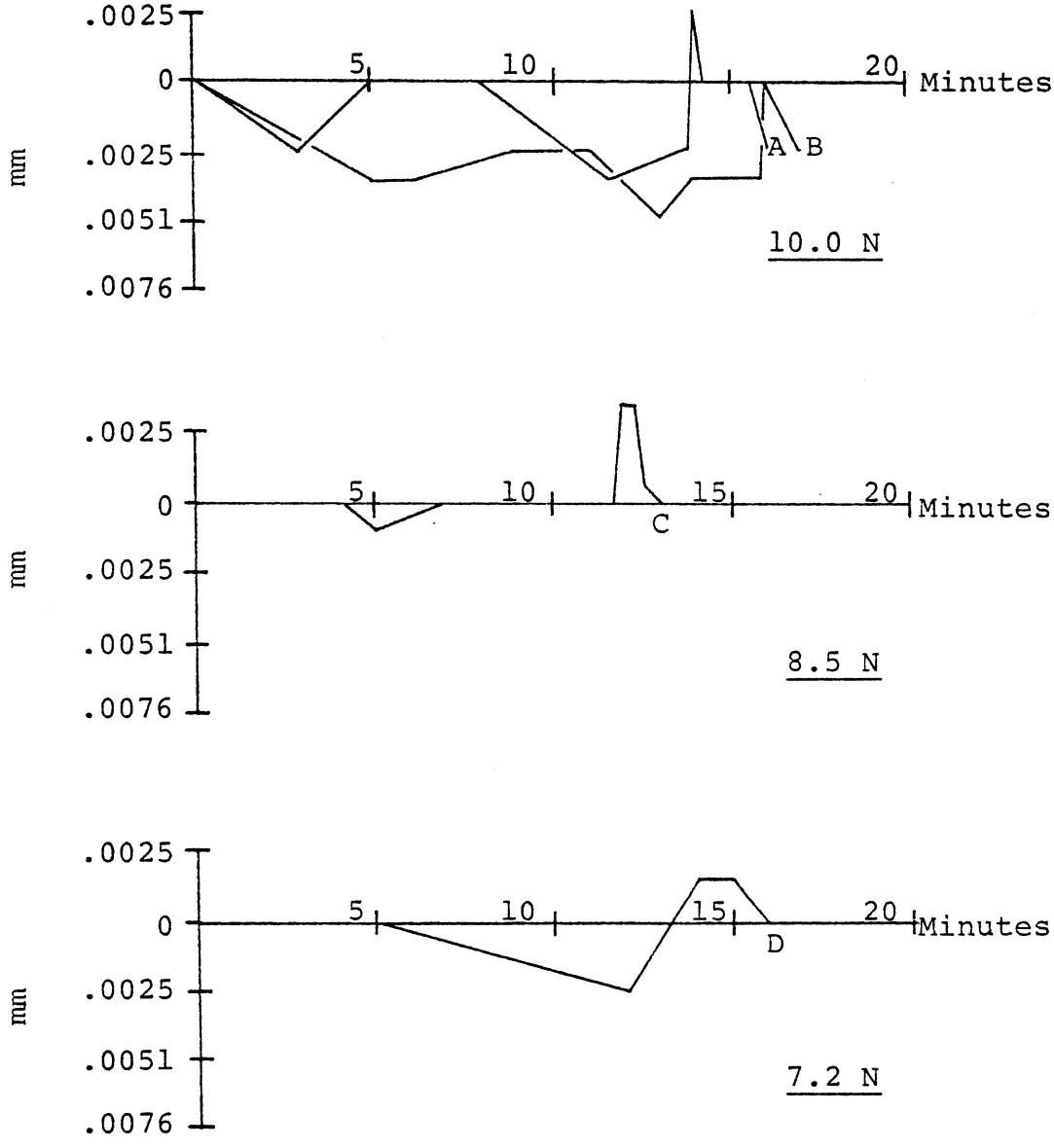

Figure 16b. Pin displacement trace for PVCT I4B in dry sliding (rigid PVC II).

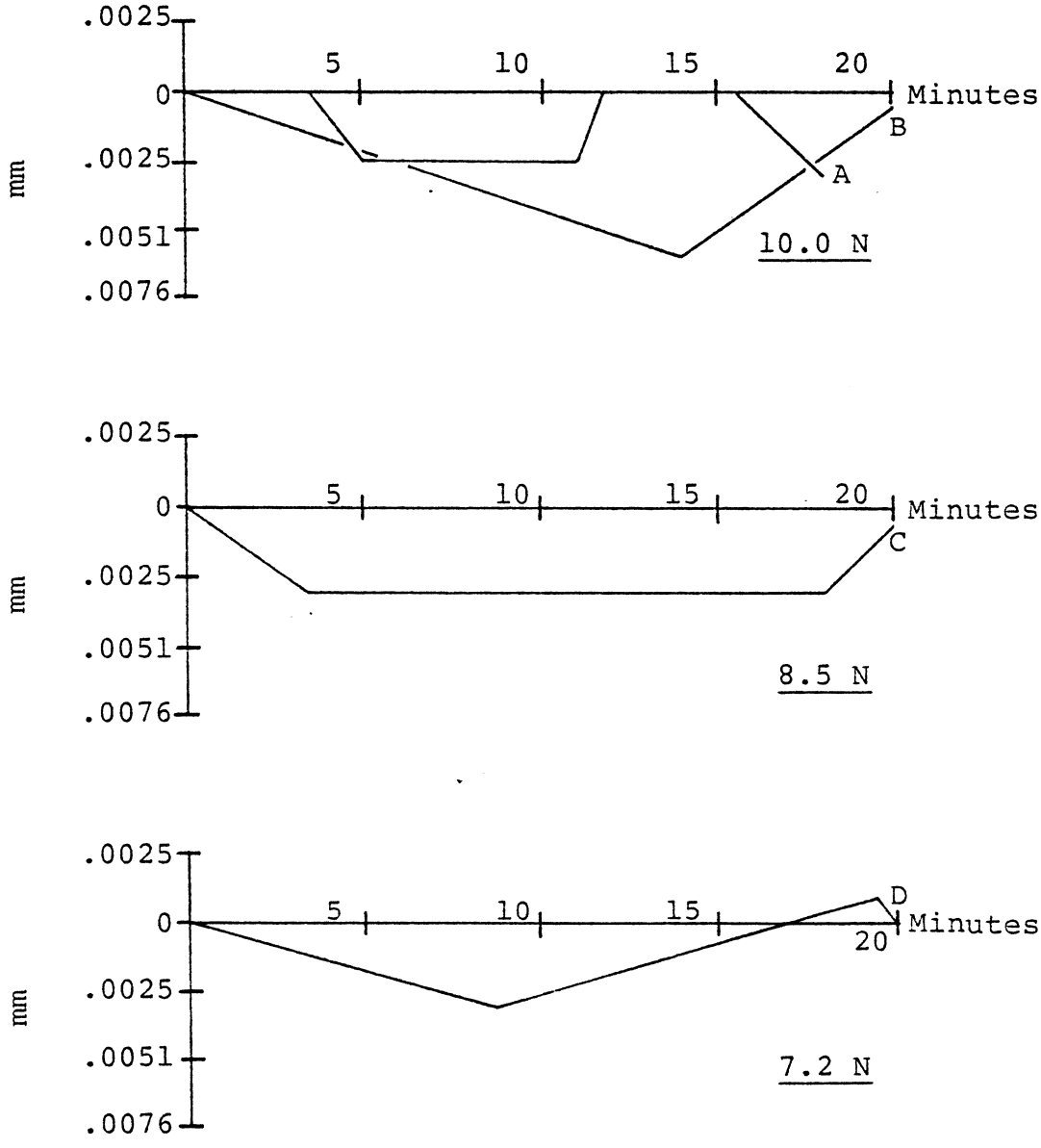

Figure 16c. Pin displacement trace for PVCO I4A in dry sliding (rigid PVC I).

In the 10 N runs of the PVC II trials, a sharp increase and decrease in pin displacement corresponded to the end of transition where the abrupt decrease in the friction force was recorded.

SEM examinations showed a flow-type of surface topography and possible evidence of delamination. Figures 17 and 18 show typical topographies for the tracks which resulted from dry sliding with a 10 N normal load. These photographs were taken from disk PVCO 15A. Figure 17 shows a possible delamination site in the second quadrant of the figure. Typical topographical structures are shown in Figure 18. Another delamination site is shown in Figure 19, where it appears that the flap covering the right hand pit has been removed and that the flap on the left hand pit was in the process of doing so. These photographs can be compared to Figure 20 which shows the wear track for the 7.2 N run in the same trial. Here there is no evidence of extreme flow or pitting. The scratch-like structure extending through several pin tracks was a prior artifact and was not caused by the sliding. The center of the photograph revealed some minor electron beam damage.

SEM photographs of this type confirmed the values of wear track depth based on the data taken from the pin displacement traces. Comparisons of penetrations recorded from the traces and those calculated from the width of the

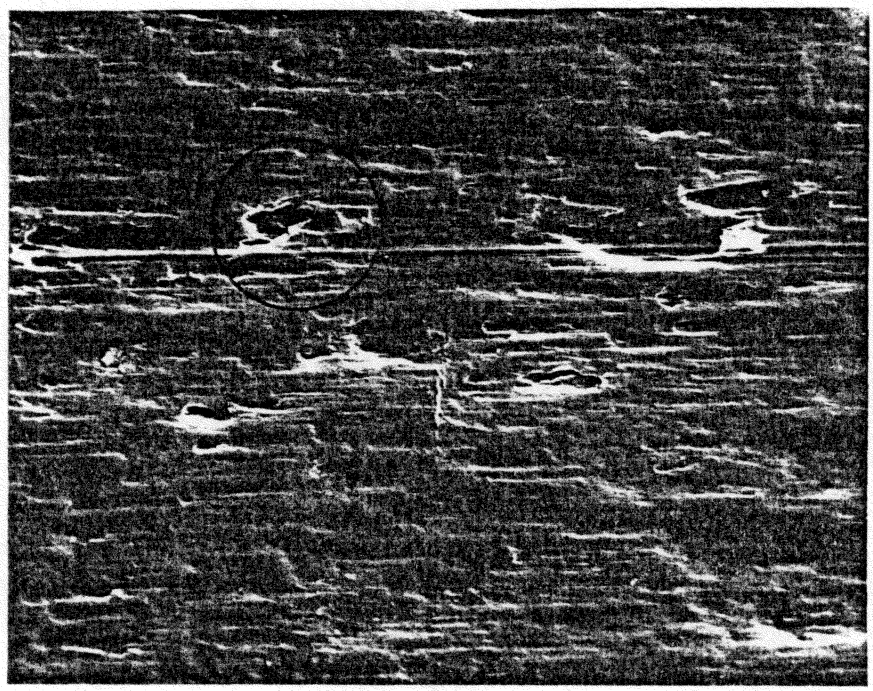

20μm

Figure 17. Wear track A for disk PVCO I5A for a 10 N normal load. Note the pit in the second quadrant (rigid PVC I-X1000).

Figure 18. Wear track B for disk PVCO 15A for a 10 N normal load (rigid PVC I-X1000).

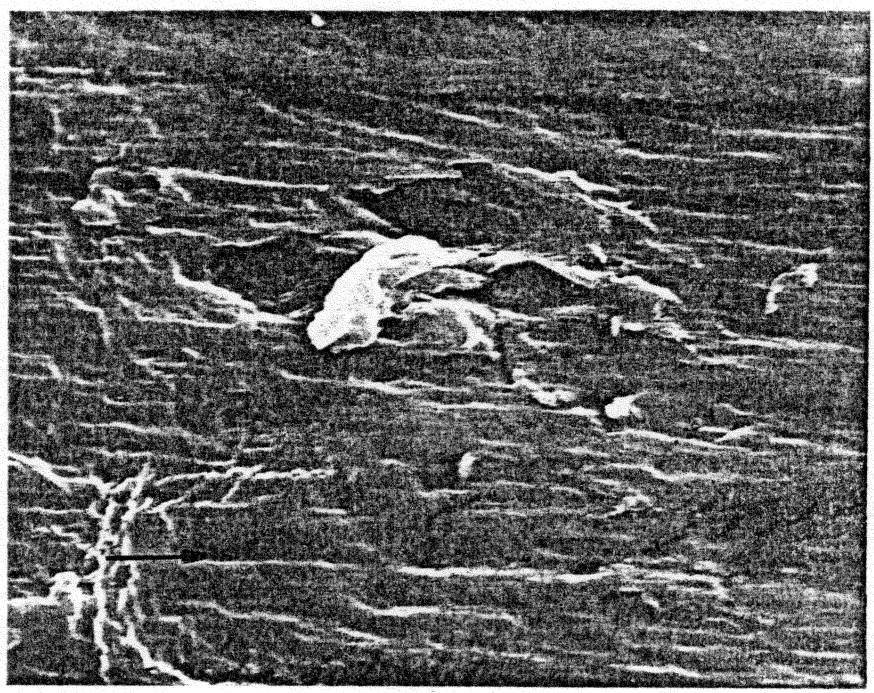

Figure 19. Delamination site in track B of disk PVCO 15A (rigid PVC I-X2000).

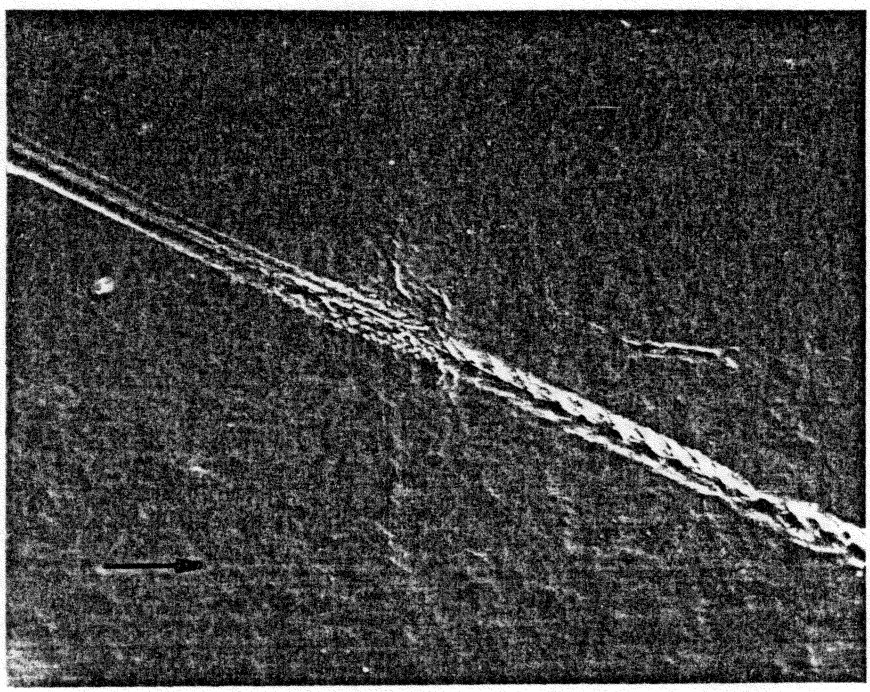

Figure 20. Wear track D for disk PVCO 15A for a 7.2 N normal load (rigid PVC I-X1000).

track generally showed correlations within ± 0.0025 mm. Although the method used to calibrate the pin displacement was not sophisticated, the results showed that the procedure was adequate and that the traces accurately reflected the actual pin penetration. An attempt to measure the maximum wear track depth by taking a transverse cut across the crosssection was not successful. The cut was attempted on an Isomet diamond abrasive saw, but as shown in Figure 21, a rough burr obscured the edge of the wear track.

Polycarbonate

Similar dry sliding trials were conducted for PC disks. Since no significant constant friction was observed before this transition, the trials were not repeated. The friction trace for PC is shown in Figure 6A. In the 10 N normal load runs there was an immediate and rapid friction force increase to a generally stable level in the 4.5-5.5 N range. A similar trace was shown for the 7.2 N run, although the time required to reach the final level of 3.8 N was extended. The end of the rapid friction force increase coincided with a visible debris aggregate attached to the leading edge of the pin. This debris formation was also associated with an audible vibration as discussed previously. There was no consistency in the pin displacement traces for individual runs.

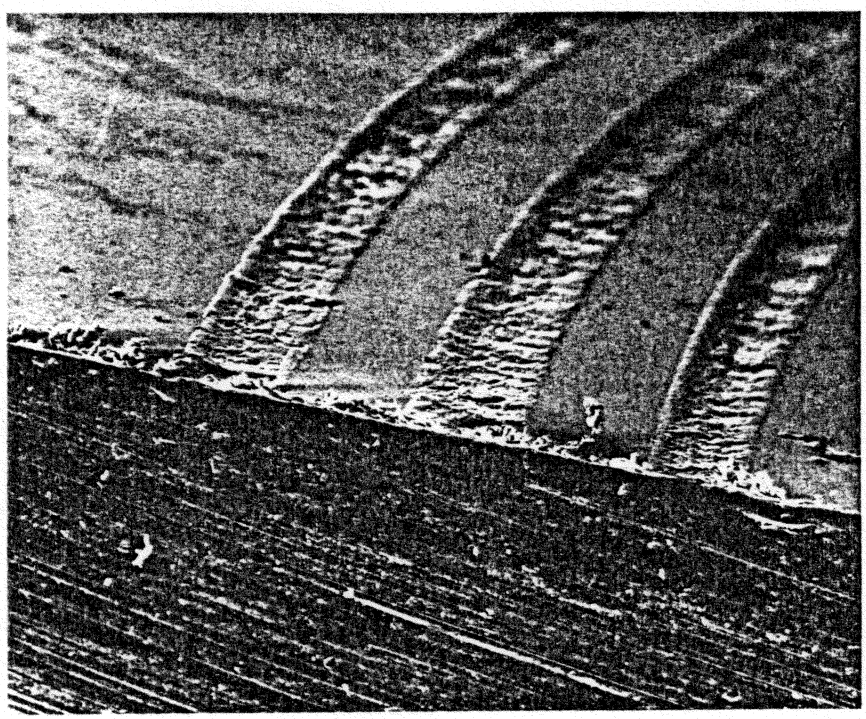

.04 cm

Figure 21. Transverse section of the wear tracks from disk PVCT 14A obscured by a burr (rigid PVC II-X50).

The wear tracks for PC, shown in Figure 22, were much smoother when compared to those produced in Rigid PVC. The scale of roughness was much finer than that observed on the PVC tracks. Figure 23 shows one of several structures found in the tracks, and appears to be a back-transfer wear debris aggregate composed of many small wear particles. Individual wear particles can be seen as small white specks on either side of the center structure.

UHMWPE

No debris production was observed throughout the trial for any normal load run. The friction traces for UHMWPE are shown in Figure 7A. In most cases there was an initial decrease in the friction force accompanying run-in, followed by a gradual increase and leveling near the initial friction level. In contrast to the other polymers the friction levels were much lower and the traces quite smooth over the length of each run.

The pin displacement trace showed that the penetration increased with sliding distance for all loads. The rate of penetration was generally higher in the first one to two minutes of sliding. An SEM photograph of the wear tracks is shown in Figure 24, and revealed no distinguishable events aside from the obvious plastic deformation. No wear debris or flow-type surfaces were visible at high magnifications.

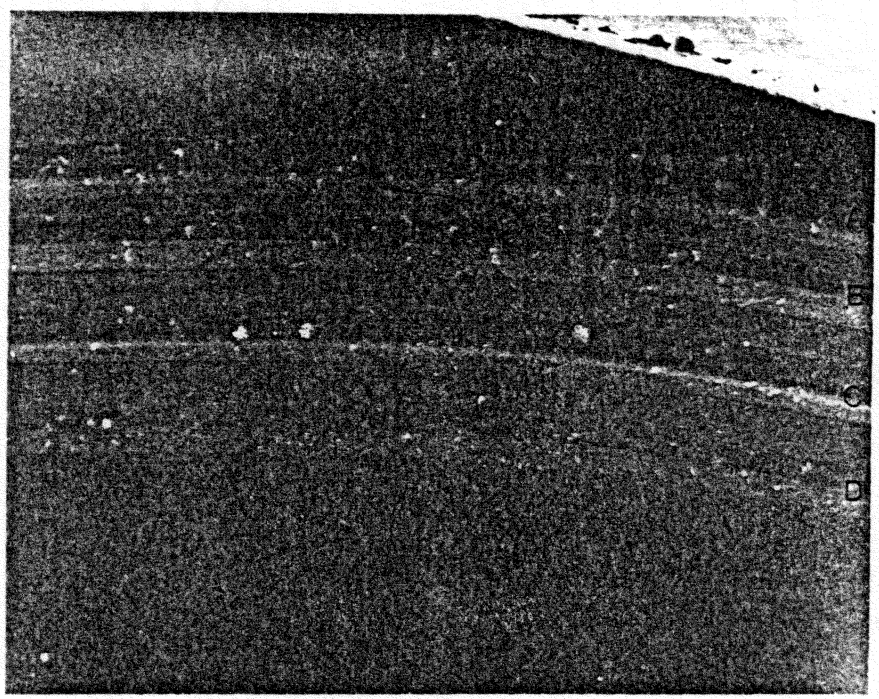

.1 cm

Figure 22. Wear tracks for disk PC IlA resulting from dry sliding (PC-20).

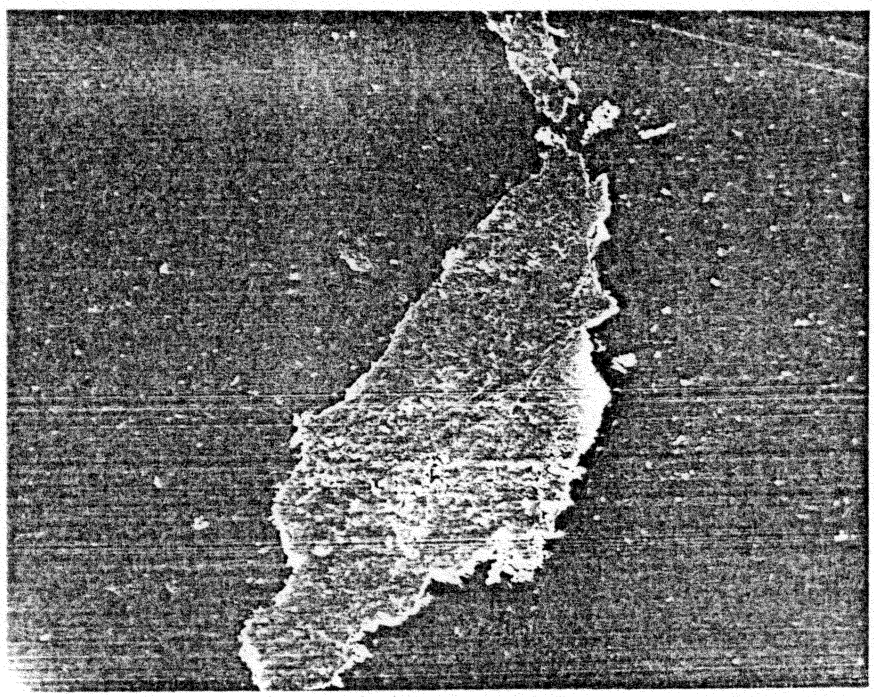

Figure 23. Detail of back-transfer to track B of disk PC IlA (PC-Xl000).

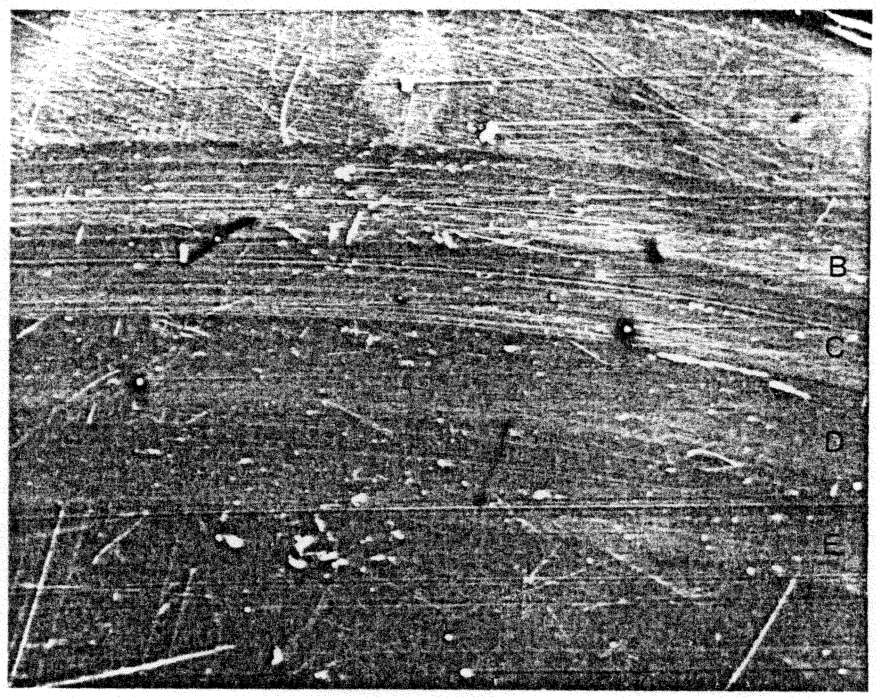

Figure 24. Wear tracks for disk UPE IlA resulting from dry sliding (UHMWPE-X20).

Interrupted Tests

Since the transition in friction of PVC was preceded by a period of constant friction, interrupted tests were undertaken to gain more information from SEM analysis of the wear tracks. One sample each of PVC I and II and PC were subject to dry sliding with a normal load of 10 N. Several runs were interrupted at points prior to and during the transition. For rigid PVC the interruptions generally occurred before transition, near the end of transition, and after the transition was complete. For PC the interruptions occurred after a certain number of cycles, i.e. 10, 25, 40, 60, and 100.

The SEM observations did not reveal any type of progressive changes from smooth to rough topography. The primary differences from track to track were their width and apparent depth. Close examination showed no cracking or surface phenomenon that could be interpreted as a fatigue mechanism. It can only be concluded that either the surfaces did not change (which is unlikely), or that the changes were not detectable with the SEM.

Summary

1. The normal loads used in the trials were sufficient to force each polymer into plastic deformation.
2. Debris was generated in the rigid PVC trials after several minutes of sliding. Debris production was

delayed in PC, but only for a limited number of cycles. No debris was produced in the UHMWPE trials.

3. The trials produced three distinct friction force traces corresponding to the three polymers tested. The PC trace was characterized by a rapid increase in friction force from the start of the trial to a relatively stable plateau. The highest friction levels were attained with PC. The rigid PVC traces had three distinct regions defined by the rate of friction force increase per unit sliding distance. The UHMWPE traces were generally flat and had significantly lower values of friction force than the other polymers.
4. Higher friction force levels were associated with higher normal loads.
5. The pin penetration curves in the rigid PVC trials showed a general trend toward penetration in Region I followed by a decrease in penetration starting at some point in the Transition Region.
6. SEM photographs of rigid PVC wear tracks showed a flow-type of surface topography and evidence of delamination wear. Similar photographs for PC and UHMWPE showed very small wear particles and no evidence of wear respectively.

Phase II - Lubricated Sliding

The purpose of this phase was to repeat the procedures of Phase I but to include a variety of simple lubricants to investigate their effect on wear, friction levels, and the friction traces established in Phase I. The amount of wear was not measured since no provisions were taken to screen the lubricant after the trial and the disks were cleaned prior to coating for SEM studies. However, wear tracks were observed for the rigid PVC and PC specimens, and were found to be similar to those for dry sliding. No debris was observed in the UHMWPE trials. These trials were run for rigid PVC II, PC, and UHMWPE at normal loads of 10.0, 8.5, and 7.2 N. None of the polymers were soluble in the lubricants.

Rigid PVC II

The most noticeable effect of lubricated sliding was the elimination of the friction force transition. This is illustrated in Figure 25, where the actual traces for the 10N normal load dry and lubricated trials are combined to show the effects of lubricant additions. Similar curves could have been developed for the other polymer/load/lubricant combinations. The data required to make these comparisons ared contained in the figures of Appendix A and tables of Appendix B. The general results are detailed below.

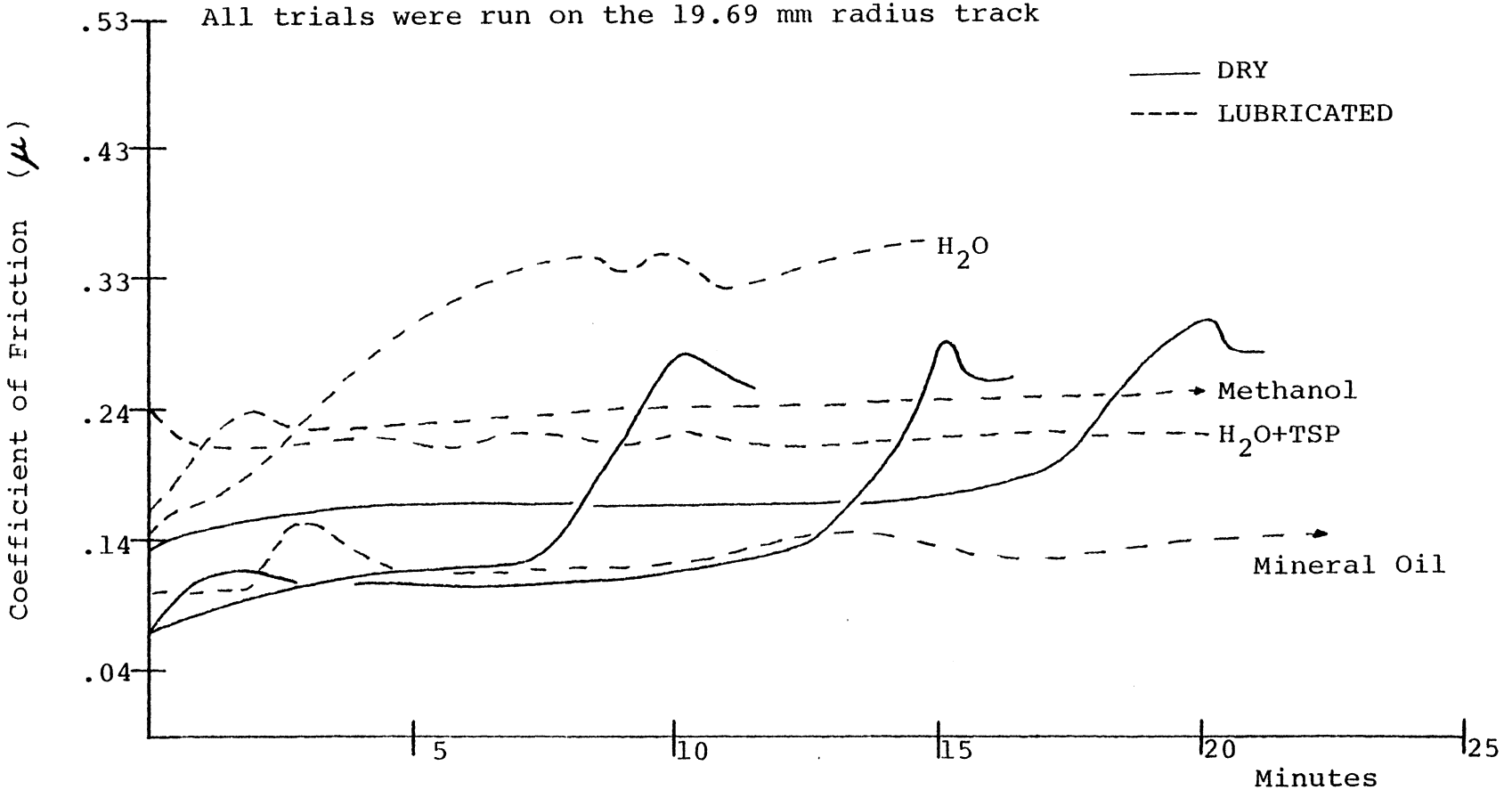

Figure 25. Friction traces for all 10 N normal load dry and lubricated sliding trials for rigid PVC II.

The water and methanol runs showed a steady rise in friction forces in the first 2-5 minutes (4.8-16 m sliding distance) to a quasi-steady level for the remainder of the trial. The friction level for the H_2O+TSP and mineral oil trials remained fairly constant throughout the run. In general, higher friction force levels corresponded to the higher normal load runs. The friction traces are shown in Figures 8A and 9A in Appendix A. The highest friction levels attained were in the 2.2-2.5 N range for water and methanol. The 0.7-0.9 N friction level associated with mineral oil was significantly lower. The addition of TSP to water resulted in a 30% decrease in friction force levels as compared to sliding in water only.

The pin displacement traces in the lubrication trial showed a steady rate of penetration. The depth of penetration was similar to the dry sliding penetration at the point when the sliding trials were terminated. Figure 26 was typical of the wear tracks for the water only runs. The flow-type topography was generally confined to a narrow band at the center of the track, and was similar to the type of surface observed in dry sliding. Outside of this band the surface appears to be smoother than that produced in dry sliding. No photographs were available for the other lubricant trials.

Figure 26. Wear track for water only sliding with a 10 N normal load (rigid PVC II-X1000).

Polycarbonate

The friction traces for PC are shown in Figures 10A and 11A. The traces showed a significant drop to lower values immediately after the start of the run followed by a gradual increase to a fairly constant level (H_2O) or a rapid increase to a fairly constant level (H_2O+TSP and methanol). The friction force was significantly lower for mineral oil trials, generally 50-75% compared to other lubricants and 70-80% lower compared to dry sliding. Higher normal loadings in lubricant groups usually resulted in higher friction force levels. The curves were similar to those for PVC II, i.e., that the final friction levels were higher for water and methanol, followed by H_2O+TSP (20% below water only), and finally mineral oil. The friction levels attained in ten minutes of sliding were lower than those steady levels in dry sliding.

With the exception of mineral oil which maintained a relatively constant penetration depth, the trend for pin displacement showed increased penetration over the length of the trial. At the point corresponding to the end of dry sliding the average displacement was deeper than the average dry sliding depth. However, the average pin depth in the lubrication trials was within the scatter of values for dry sliding after ten minutes. SEM photographs taken of the wear tracks showed no noticeable differences compared to

those for dry sliding, except for the lack of debris particles which were cleaned off prior to coating.

UHMWPE

The friction traces for UHMWPE contained in Figures 12A and 13A showed little difference from those derived from dry sliding, although the levels were generally lower. The exception was found in those 10.0 and 8.5 N normal load runs with methanol where a comparatively large increase in friction was recorded. This increase was not observed for the 7.2 N run. The ranking of the final friction levels for each lubricant was the same as the previous trials. The friction level of H_2O+TSP was 26% less than water at the point where the run was terminated.

Each pin displacement curve was marked by a rapid penetration of the pin in the first one to two minutes of sliding, followed by a smooth and gradual penetration (H_2O), or a stable pin position (H_2O+TSP, methanol, and mineral oil).

An SEM examination of the wear track from the H_2O run indicated a rougher surface topography than previously documented in dry sliding. This is illustrated in Figure 27. The unworn surface was rougher than the wear tracks. A similar surface was noted on the methanol disk, but was not seen in the dry sliding disk. It cannot be said with certainty whether this surface was a prior condition or if it

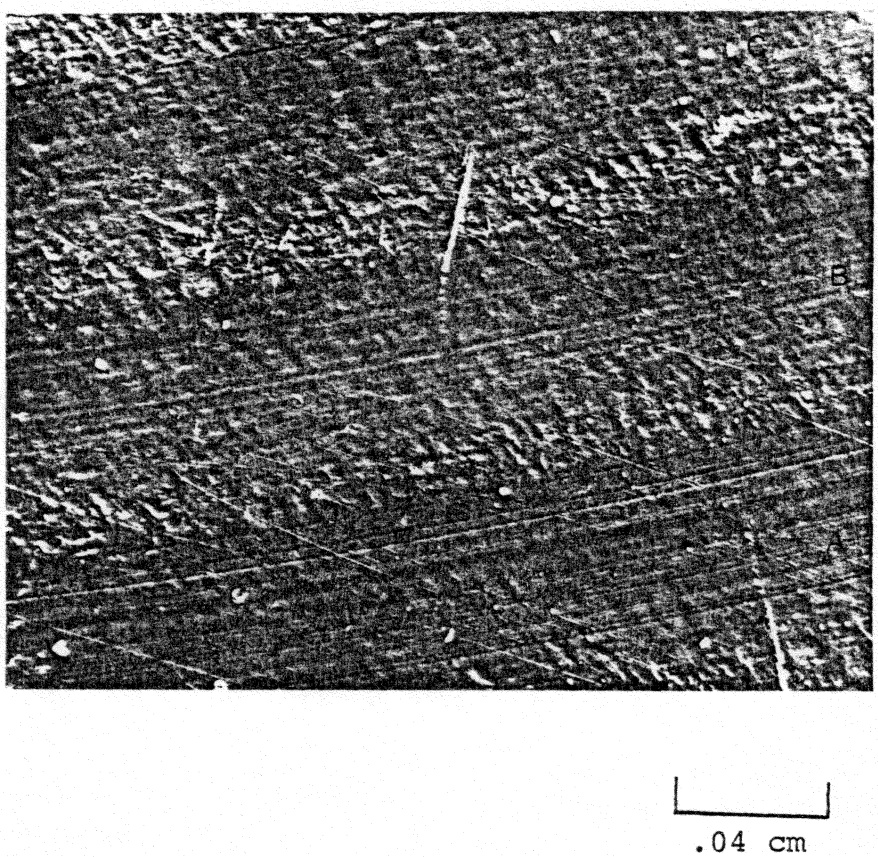

Figure 27. Wear track topography for water only sliding (UHMWPE-X50).

was produced via absorption. It is known that the percent water absorption is less in UHMWPE than in PC and rigid PVC (26). No similar structures were seen on the other polymer disks. The author feels that this surface was a prior artifact confined to the disks used in this portion of the investigation.

Summary

1. The presence of a lubricant fundamentally altered the friction force curve for PC and PVC II. The PC trace was characterized by a significant drop in the friction level followed by an increase to a higher value. The rapid transition in the friction in PVC II was replaced by either a steady rise in force in the first minutes of sliding, followed by a quasi-steady level (H_2O and methanol), or the traces remained fairly level throughout the trial (H_2O+TSP and mineral oil). No significant differences were noted for UHMWPE except for a steady rise recorded with the methanol.
2. The final friction force levels were reduced as compared to dry sliding and higher normal loads produced higher friction traces.
3. Regardless of polymer, the highest friction levels were obtained from the water only and methanol trials. The friction levels produced with H_2O+TSP

runs were consistently 20-30% below that produced for water only. The friction forces developed in sliding with mineral oil were significantly lower than any other lubricant.

4. The pin penetration traces were more uniform in their displacement as compared to dry sliding. For PC and PVC II the depths of penetration were consistent with the values in dry sliding at the point where the dry sliding trials were terminated. The pin penetration for UHMWPE was generally less in these trials with the exception of the water only runs.

DISCUSSION

Fatigue in Dry Sliding

Of immediate interest to this investigation is whether the data derived from these experiments confirm the existence of a fatigue wear mechanism. The most obvious evidence of a fatigue mechanism was the delay in the development of debris until after several minutes of dry sliding in the rigid PVC trials. Debris production was also delayed in the dry sliding PC trials. A rapid increase in friction force coincided with debris production in both cases. In the rigid PVC trials, the friction curve was composed of three regions characterized by the rate of friction force increase. The possibility of a fatigue mechanism demonstrated by this type of data was first proposed by Dowson (27).

The results from the friction and pin displacement traces indicated that the pin penetrated into the polymer in a run-in mode and that the process associated with penetration is plastic deformation. Once past the brief, sharp rise in friction force level from the start of the run, the more gradual increase in friction probably resulted from continued ploughing, although it seemed that this occurred at a reduced rate possibly reflecting reduced pressure via the development of a larger bearing area surface as a groove was formed.

In the transition region a significant increase in the friction force was recorded and the pin penetration either reversed or remained constant through the remainder of the region. The damage could be related to the growth of surface cracks causing the surface of the wear track to become rougher though this could not be verified in the SEM from the interrupted trials. A friction increase could also have resulted from thin-film transfer to the pin resulting in polymer-on-polymer sliding. In this case the friction would be expected to increase because of the added adhesion force between the polymers. However, this could not be verified since the pin was not studied for thin-film transfer and was cleaned after each run.

A comparison of the PVC composite traces showed that this transition occurred in PVC I at a shorter period of time (sliding distance) than for PVC II although the friction levels at transition were roughly the same for both polymers. A possible explanation for this phenomenon might be found in the concept of stress relaxation behavior of viscoelastic materials modeled by the Maxwell Element. Dieter (28) outlined a derivation of shear stress where:

$$\tau = G \gamma_0 e^{-t/\lambda_R}$$

Where: τ = shear strees (in tension)

G = modulus of elasticity in shear

γ_o = instantaneous eleastic strain

t = time

γ_R = relaxation of time

If relaxation time is greater for the higher molecular weight polymer, the modulus of elasticity is considered the same, and the conditions of the trial (i.e. loading, temperature, speed) are identical, then the shear stress for rigid PVC I would be greater. The greater relaxation time for rigid PVC I might have led to a higher level of retained energy as the polymer failed to return to its lowest energy state before the next loading cycle. Higher damping could accelerate a fatigue failure through thermal softening. Since this effect would be more pronounced in the region of high shear below the surface of the polymer, it would not affect the friction force level.

Since the coefficient of friction at transition was very similar, the mechanism to "trip" the transition was probably more closely allied with the friction level. If true, then a mechanism to allow fatigue failure would have a "threshold" level related to friction, below which cumulative damage leading to fatigue failure would not occur.

The mechanism by which wear particles formed could be explained through delamination theory. Suh (29) proposed

that delamination, which was a process involving plastic deformation followed by crack nucleation and propagation, would apply to thermoplastics that had inclusions that served as nucleation sites. The author proposes that the "threshold level" of friction would be the point where the trailing tensile field of the slider increased enough to promote subsurface crack propagation. The author had no evidence of the existence of inclusions, but SEM photographs taken of the wear track showed pitting sites that could be interpreted as delamination.

The pin displacement in the transition region could be explained by the initiation of pitting causing the slider to ride over a rougher surface, or by wear debris being generated to increase the bearing surface and thus reduce penetration. The friction level would increase by the added component of the ploughing. A slider riding over a pitting site would put a high stress on the crack root and promote site failure. Because of stress concentration at the tip of the root, it is reasonable to assume that any reduction in pressure caused by the slider having a greater bearing area would not have a great effect on the cumulative damage caused in later cycles.

The progression in cumulative damage as described above could not be verified in the SEM from the interrupted tests. This does not necessarily disprove the mechanism since wear

particles were removed prior to coating and sub-surface cracking would not be visible in any event. The dry sliding trials did show that visible wear particles on the leading edge of the slider were apparent by the end of transition.

The highest friction forces in the dry sliding experiements were obtained for PC. Wear particles were first noticed just prior to the friction trace becoming stable. Experiments have been conducted to verify the existence of a fatigue mechanism in PC. Rabinowitz and Beardmore (30) discerned four regimes of cyclic stress-strain behavior at ambient temperature conditions: an incubation period where the stress-strain response from the first cycle is unchanged, a transition stage where the peak stress decreases rapidly in both tension and compression, a steady state region when a new stress-strain relation remains fairly constant, and finally a region where crack propagation is followed by fatigue failure. The transition from the first to the second regime was described as a decrease in resistance to plastic strain, or thermal softening.

The actual friction trace for PC did not suggest that these four regimes were occurring; however, the investigators suggested that the incubation period would be eliminated entirely if a sufficient population of defects existed prior to cycling, leading to immediate cyclic

softening. Further, the transition region is short for ductile polymers such as PC. The curves generated in the dry sliding experiments did not suggest a steady state regime after transition, but that a steady friction force coincided with visible debris formation, inferring that the polymer went directly from transition to crack propagation and surface failure.

The UHMWPE samples did not display a fatigue mechanism in the sense of debris production, but an argument could be made for its failure in gross plastic deformation. The friction levels obtained in these trails were significantly lower than both PC and rigid PVC, and the depth of penetration was greater. Fatigue wear has been described for HDPE under conditions more severe than imposed in these trials (31).

Since the three thermoplastic polymers exhibited different friction force behavior under the same experimental conditions, a "threshold level" of friction as proposed for rigid PVC might exist for the other two polymers. This level would have been exceeded immediately by the conditions imposed in the polycarbonate runs, and not attained in UHMWPE under the same trial conditions. This assumption can only be valid if the same or similar type of failure process existed in all three polymers.

It should be noted that the percent crystallinity of

the polymer increased from PC (low) to UHMWPE (high). Since the general friction levels increased and the proposed "threshold level" of friction was more apparent with decreased crystallinity, it is possible that some relationship existed between crystallinity and the fatigue process. However, the author was unable to verify the existence of this relationship in the literature.

Lubrication Effects

The general effect of introducing a lubricant to the sliding system was to decrease the measured friction and alter the configuration of the traces. Its effect on the rate or amount of wear was not measured, although similar wear track topographies were observed in both dry and lubricated trials. The pin penetration was roughly the same for both at the point where the dry sliding trials were terminated, except in UHMWPE where the pin penetration was less with the H_2O+TSP, methanol, and mineral oil.

The final friction levels were consistently highest for water only and methanol, and lowest for mineral oil. The low level for mineral oil was not surprising since it had been calculated potentially to provide thin film lubrication. The viscosities of the other lubricants were roughly equivalent and not expected to provide a thin film layer between pin and polymer, but the H_2O+TSP friction level was consistently lower than water only and methanol.

The reason for the lower friction level might have been the surfactant provided in the "spic and span" formulation to reduce surface tension and improve wettability. Surfactants have been shown to reduce friction (32). On the other hand, the addition of trisodium phosphate alone might have been responsible for this behavior.

If the primary effect of the lubricant was to reduce friction below the "threshold level", then it is possible that some other wear process other than fatigue occurred. The reduction in friction would reduce the trailing tensile field, however since the pin displacement traces showed continuous plastic deformation over the length of the trial, it would be expected that any voids or inclusions would still serve as nucleation sites. If cracks were to form and propagate to the surface of the polymer then wear debris would eventually be produced. It has been proposed that the presence of a lubricant might accelerate the cumulative damage if the lubricant was trapped in the crack and hydrostatic forces were introduced causing higher stresses at the crack tip.

Abrasion/Fatigue Model

Based on the results of this work, the author proposes the following model of fatigue wear for a polymer sliding on a machined metal surface, and the manner in which it arises from abrasion. This model incorporates several wear

theories which have been detailed and referenced in the previous sections.

During abrasive run-in a penetrating asperity will produce wear debris. Some of the debris, and other debris that are transported to the site, tend to accumulate on the leading edge of the asperity forming an aggregate mass. With continued sliding this mass can alter the profile of the asperity causing the flank angle to be less than the shear angle of the particular contacting polymer. The aggregate mass also provides greater bearing area to reduce asperity penetration. When the asperity can no longer function as a cutter, polymer deforms elastically and plastically over and around the asperity giving rise to a steady state regime in fatigue wear that would continue until the aggregate mass extruded from the asperity and abrasive wear resumed. The mechanism that causes extrusion is not known, but is probably caused by a combination of factors resulting from loading, traction, topography, and debris transport conditions.

During the steady state mode a fatigue mechanism would begin to take effect as a result of plastic cycling. This fatigue mechanism would be modeled after Delamination Theory and relies on the presence of voids and inclusions to nucleate subsurface cracking. Further cycling would cause the cracks to propagate and eventually migrate to the

surface leading to pitting and debris production.

The subsurface cracking would not propagate unless a certain "threshold level" of friction existed which would be determined by polymer material and crystallinity, loading, speed, temperature, and lubrication. The use of an effective lubricant would delay crack migration, but accelerate particle production if a surface crack formed. These particles would either be transported out of the system or accumulate at other asperity sites and affect the wear mode.

If the process goes to steady-state as some of the data indicates, it may help to explain why material worn abrasively can reach a level of steady volume loss after run-in. Thus, the author perceives wear in metal/polymer systems as a dynamic process where the elements of abrasion and fatigue manifest themselves continously depending on the conditions at the time.

CONCLUSIONS

The results contained in this work indicate that a fatigue mechanism appears to exist in a metal-on-polymer dry sliding system. In-situ SEM abrasive wear experiments showed that wear particles were formed and collected at asperities into an aggregate mass that altered the subsequent wear process through load support and modification of the effective asperity geometry. Further, the extrusion of the aggregate perpendicular to the direction of sliding suggested a continuing dynamic process of abrasive wear. It was concluded that if a fatigue mechanism was to become a significant wear mode it must occur after run-in, at which time abrasive effects have been reduced by eliminating abrasive wear sites through debris buildup or transport.

Dry and lubricated sliding trials of a metal pin on polymer disks were conducted with provisions to minimize abrasive and temperature effects. Adhesive effects were to be demonstrated with a comparison between dry and lubricated sliding. These tests were conducted with three types of thermoplastics; PC (amorphous), rigid PVC (semi-crystalline), and UHMWPE (highly crystalline). With the same loading and speed conditions, the higher friction levels corresponded with reductions in polymer crystallinity.

In the rigid PVC and PC dry sliding trials, wear

particles were not generated immediately, but rather were observed after several minutes (rigid PVC) or several cycles (PC) of sliding. A transition to the highest friction levels coincided with debris formation. No wear debris was observed from the UHMWPE trials, and the friction force trace was flat and well below the levels recorded with the other polymers. The rigid PVC materials exhibited three distinct regions corresponding to the rate of friction force increase. The transition to a higher rate occurred at nearly the same friction level, although the transition occurred sooner for the higher molecular weight rigid PVC I. Thus the level of friction was considered fundamentally important in determining the point where the rate of friction force increase accelerated, and it was proposed that this "threshold level" existed for each polymer.

It was concluded that under the loading and speed conditions of the trial, PC was above the "threshold level" while UHMWPE was below. Wear particles were thought to form because of a delamination wear mechanism, and was confirmed to some extent by the presence of pitting in the wear tracks of rigid PVC. The lubricants had a profound effect on the level of friction and the configuration of the trace, but since plastic and elastic deformation continued to occur during the trial it was considered likely that the delamination mechanism continued to operate, if at a reduced rate.

The volume of wear could not be verified in either trial due to the testing procedures used.

A qualitative model relating the observations of abrasive wear and the experiments of fatigue wear was developed. This model proposed a manner in which a fatigue mechanism could operate in steady state abrasive wear.

RECOMMENDATIONS

The author feels that the results of this work are significant enough to warrant additional investigation in several areas, including:

1. The study of voids and inclusions in the polymer.
2. Careful investigation of the wear tracks prior to debris generation by mounting polished transverse sections and locating sub-surface cracking to verify the delamination mechanism.
3. Additional studies of lubrication effects particularly the role of surfactants to reduce surface traction. These studies might include water and surfactant solutions only.
4. Transport and deposition using radioactive tracing techniques to study the formation of debris aggregates and its effect on run-in and steady state abrasive wear.
5. Modeling of debris aggregates and investigation of their role in asperity modification and load bearing.

The procedures used in this work showed several shortcomings. In particular the experience with in-situ SEM studies showed that observations of polymer wear were severely limited by particle charging, electron beam damage, and restricted view of the wear process. Also, cleaning and coating polymer samples eliminated important data on debris

disposition. It is recommended that an optical procedure be used to investigate the wear process as it occurs. Fiber optics might have some application here.

It is expected that the experiments should be repeated under more carefully controlled circumstances. Although the author did not perform these experiments in a reckless manner, a more systematic program employing a variety of polymers particularly suited for bearing applications could provide a superior data base from which a more in-depth statistical analysis could be performed and more specific conclusions drawn.

Longer run times in dry sliding would be helpful in determining what happens in the wear process after transition. Also, few conclusions about the differences in the amount of wear between dry and lubricated sliding could be gathered since the lubrication trials were usually much longer in duration. If trials of the type outlined in the previous sections are contempleted, the sliding times should be identical. It would also be helpful to collect and analyze the wear debris produced. This might offer a better insight into relative volumes of wear and the manner in which they were produced.

REFERENCES

1. Eiss, N.S., The Wear of Polymers by Transfer to Hard, Rough Surfaces, Final Report, Virginia Polytechnic Institute and State University, 1981.

2. Warren, J.H., The Prediction of Polymer Wear Using Polymer Mechanical Properties and Surface Characterization Parameters, Doctoral Dissertation, Virginia Polytechnic Institute and State University, August, 1976.

3. Herold, J.H., A Model for Abrasive Polymer Wear, Doctoral Dissertation, Virginia Polytechnic Institute and State University, June, 1980.

4. Sarkar, A.D., Wear of Metals, Pergamon Press, New York, 1976.

5. Archard, J.F., "Contact and Rubbing of Flat Surfaces", Journal of Applied Physics, Vol. 1, No. 6, 1953, pp. 981-988.

6. Bowden F.P. and D. Tabor, The Friction and Lubrication of Solids - Part 1, Oxford University Press, 1954.

7. Suh, N.P., "The Delamination Theory of Wear", Wear, Vol. 25, 1973, pp. 111-124.

8. Dowson, D., J. Atkinson and K. Brown, "The Wear of High Molecular Weight Polyethylene with Particular Reference to its Use in Artificial Human Joints", Advances in Polymer Friction and Wear, L.H. Lee, Ed., Vol. 5B, Plenum Press, New York, 1974, pp.

9. Crawford, R. and P.P. Benham, "Cyclic Stress Fatigue and Thermal Softening Failure of a Thermoplastic", Journal of Material Science, Vol. 9, No. 1, 1974, pp. 18-28.

10. Rabinowitz, S. and R. Beardmore, "Cyclic Deformation and Fracture of Polymers", Journal of Material Science, Vol. 9, No. 1, 1974, pp. 81-99.

11. Jain, V.K. and S. Bahadur, "The Development of a Wear Equation for Polymer-Metal Sliding in Terms of Fatigue and Topography of Sliding Surfaces", Wear of Materials - 1979, ASME, New York, pp. 556-562.

12. Jain, V.K. and S. Bahadur, "Experimental Verification of a Fatigue Wear Equation", Wear of Materials - 1981, ASME, New York, pp. 241-253.

13. Herold, loc. cit.

14. Rabinowitz, loc. cit., p. 87.

15. Jain, V.K. and S. Bahadur, "The Development of a Wear Equation for Polymer-Metal Sliding in Terms of Fatigue and Topography of Sliding Surfaces", Wear of Materials - 1979, ASME, New York, p. 557.

16. Machine Design - 1983 Materials Reference Issue, Vol. 55, No. 8, Penton/IPC, Inc., Cleveland, April 14, 1983, p. 166.

17. Ibid., p. 87.

18. Machine Design, loc. cit., p. 178.

19. Modern Plastics Encyclopedia, J. Agranoff, Ed., McGraw Hill, New York.

20. Vincent, G.S., The Effects of Molecular Weight, Surface Roughness, and Sliding Speed on the Friction and Wear of Polyvinyl on Steel, Master's Thesis, Virginia Polytechnic Institute and State University, March, 1980.

21. CRC Handbook of Applied Engineering Science, Second Ed., CRC Press, Inc., 1976, p. 140.

22. Shigley, J.E., Mechanical Engineering Design, Third Ed., McGraw Hill, Inc., New York, 1977, p 77.

23. Boresi, A.P., O.M. Sidebottom, F.B. Seely, and J.O. Smith, Advanced Mechanics of Materials, Third Ed., John Wiley and Sons, Inc., 1978, p. 619.

24. Cameron, A., Principals of Lubrication, Longman Green and Co., Ltd., London, 1966, p.811.

25. Dowson, D., "Transition to Boundary Lubrication from Elastohydrodynamic Lubrication", ASME Boundary Lubrication: An Appraisal of World Literature, ASME, New York, p. 239.

26. Machine Design, loc. cit., p. 179

27. Dowson, et. al., loc. cit.

28. Dieter, G.E., Mechanical Metallurgy, Second Ed., McGraw Hill, Inc., New York, 1976, pp. 314-317.

29. Suh, N.P., "An Overview of the Delamination Theory of Wear", Wear, Vol. 44, 1977, p. 13.

30. Rabinowitz, loc. cit.

31. Bahadur, S. and V.K. Jain, "An investigation of the Markings on Wear and Fatigue Fracture Surfaces", Wear of Materials - 1981, ASME, New York, pp. 707-713.

32. From a conversation with J. Tellmann (Manager of Technical Resources - Capital Magnetic Products Division), Capital Industries, May 22, 1983.

APPENDIX A

FRICTION TRACES

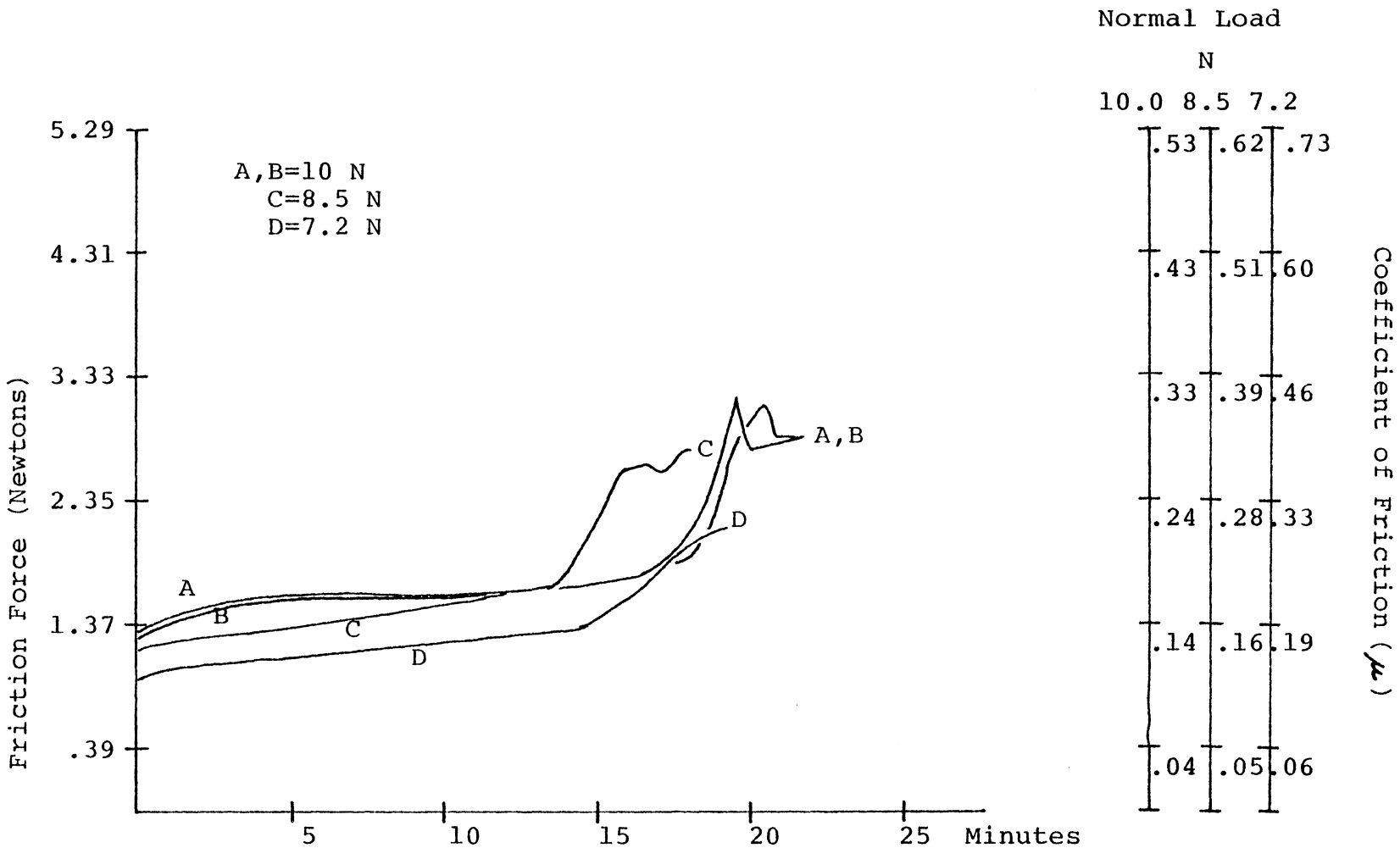

Figure 1A. Friction trace for trial PVCT I3A-rigid PVC II in dry sliding.

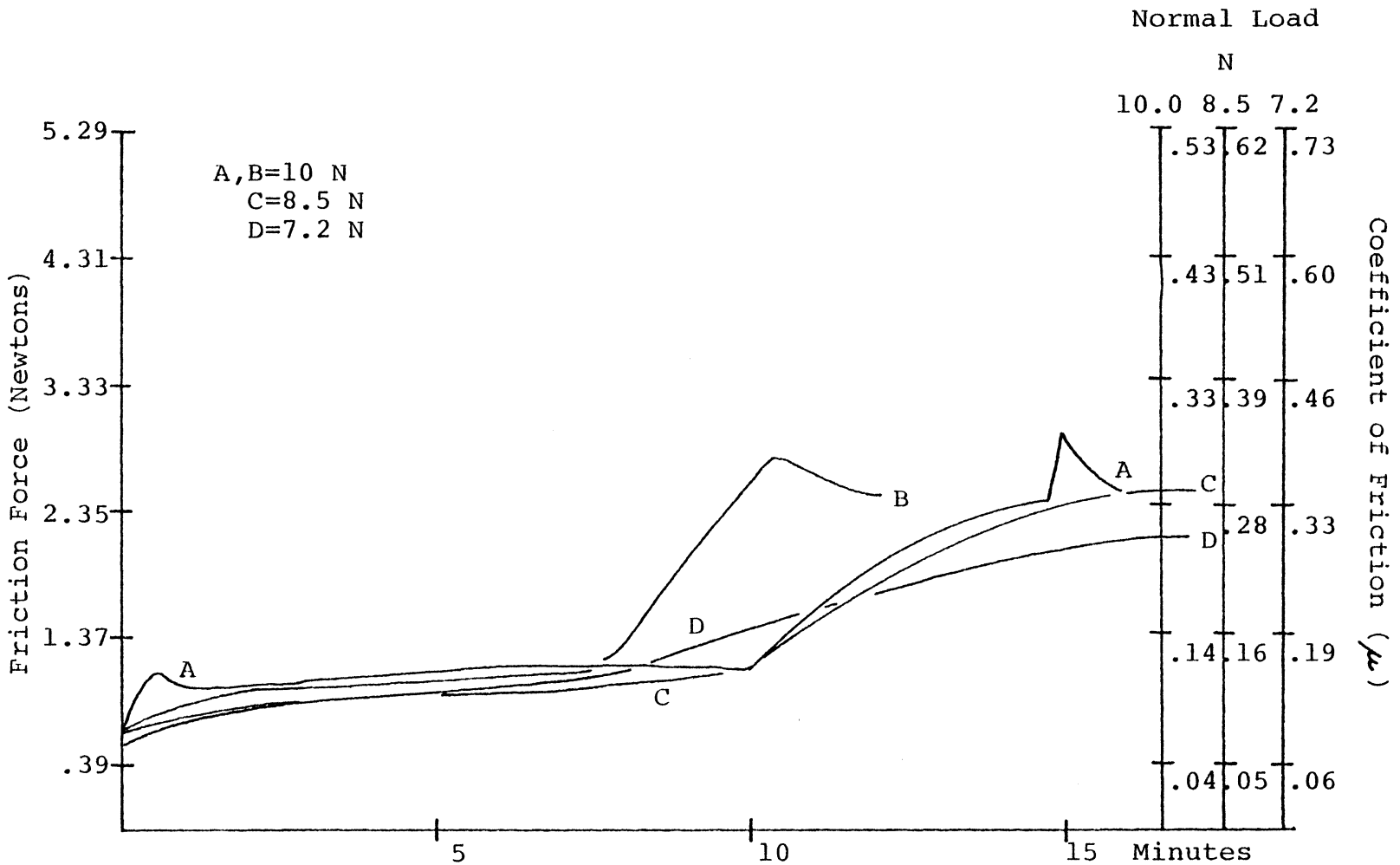

Figure 2A. Friction trace for trial PVCT I4A-rigid PVC II in dry sliding.

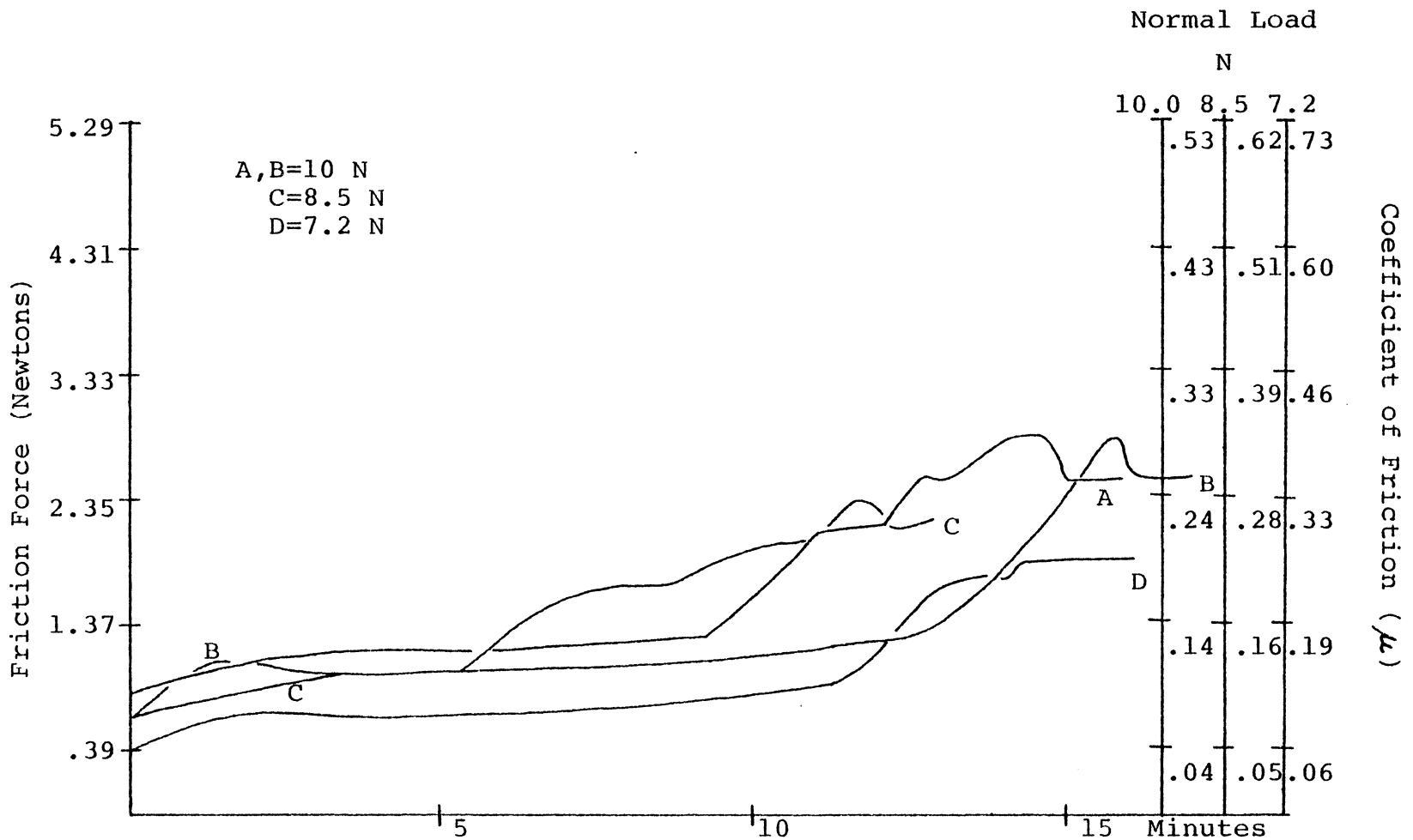

Figure 3A. Friction trace for trial PVCT I4B-rigid PVC II in dry sliding.

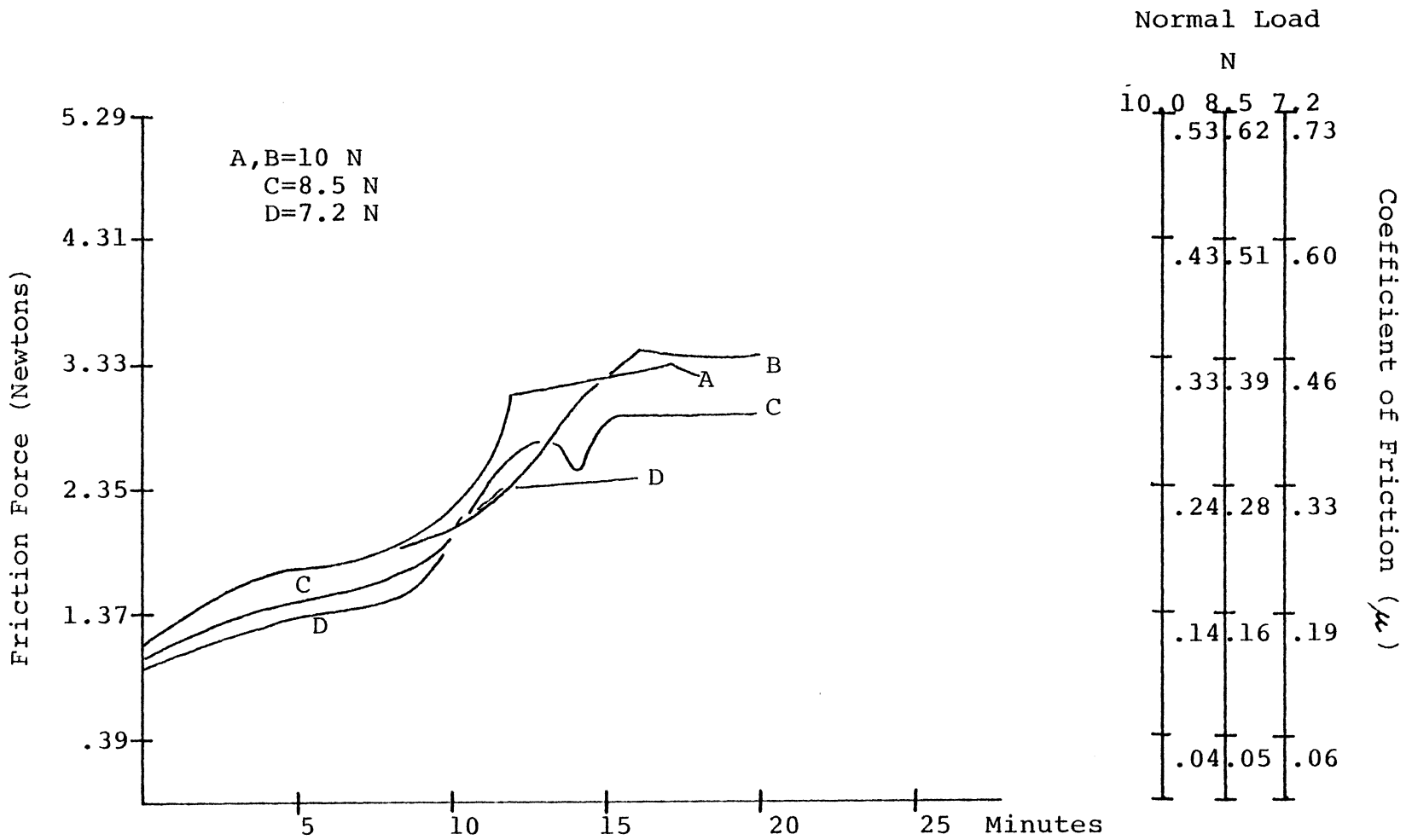

Figure 4A. Friction trace for trial PVCO I4A-rigid PVC I in dry sliding.

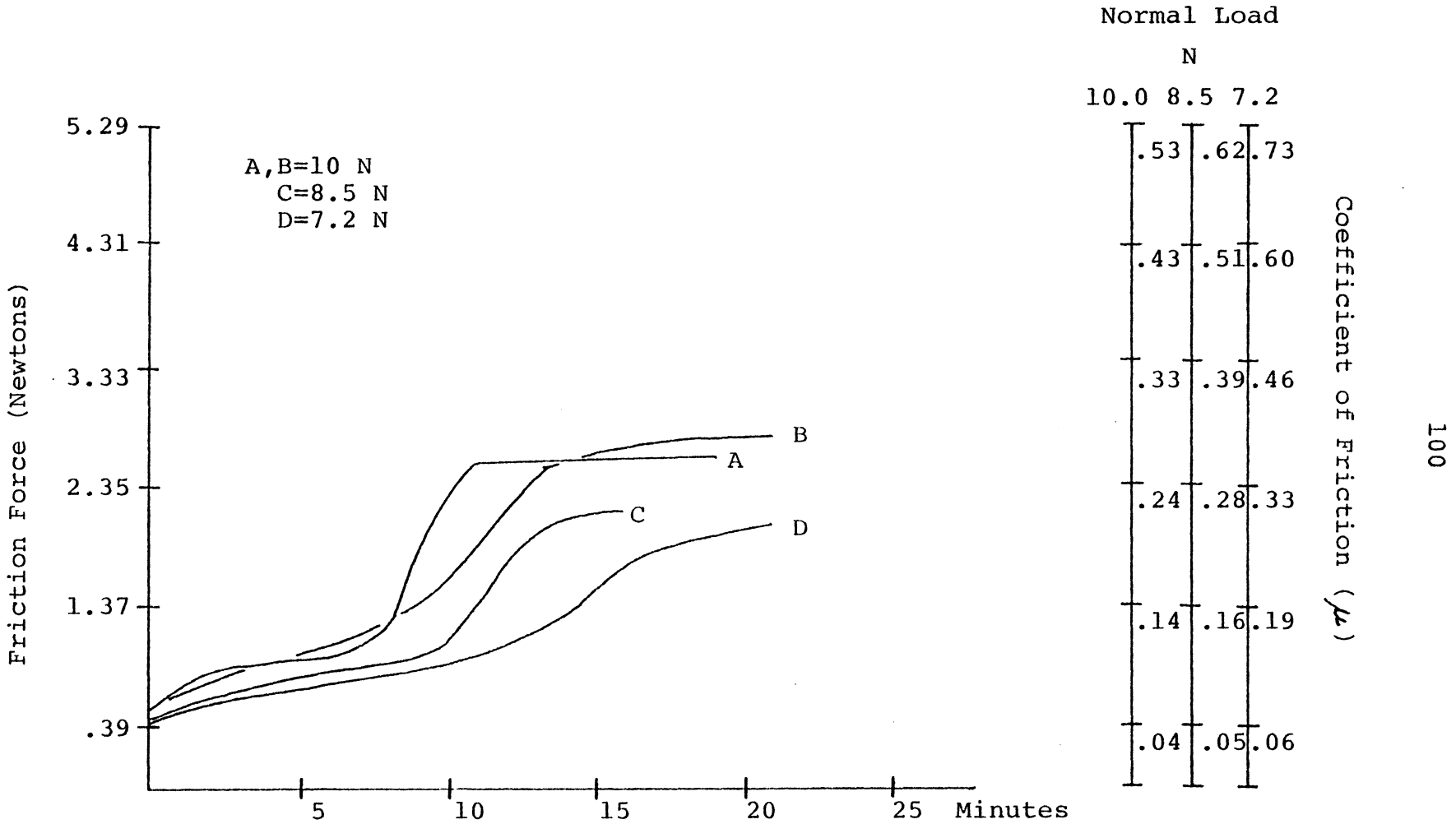

Figure 5A. Friction trace for trial PVCO I5A-rigid PVC I in dry sliding.

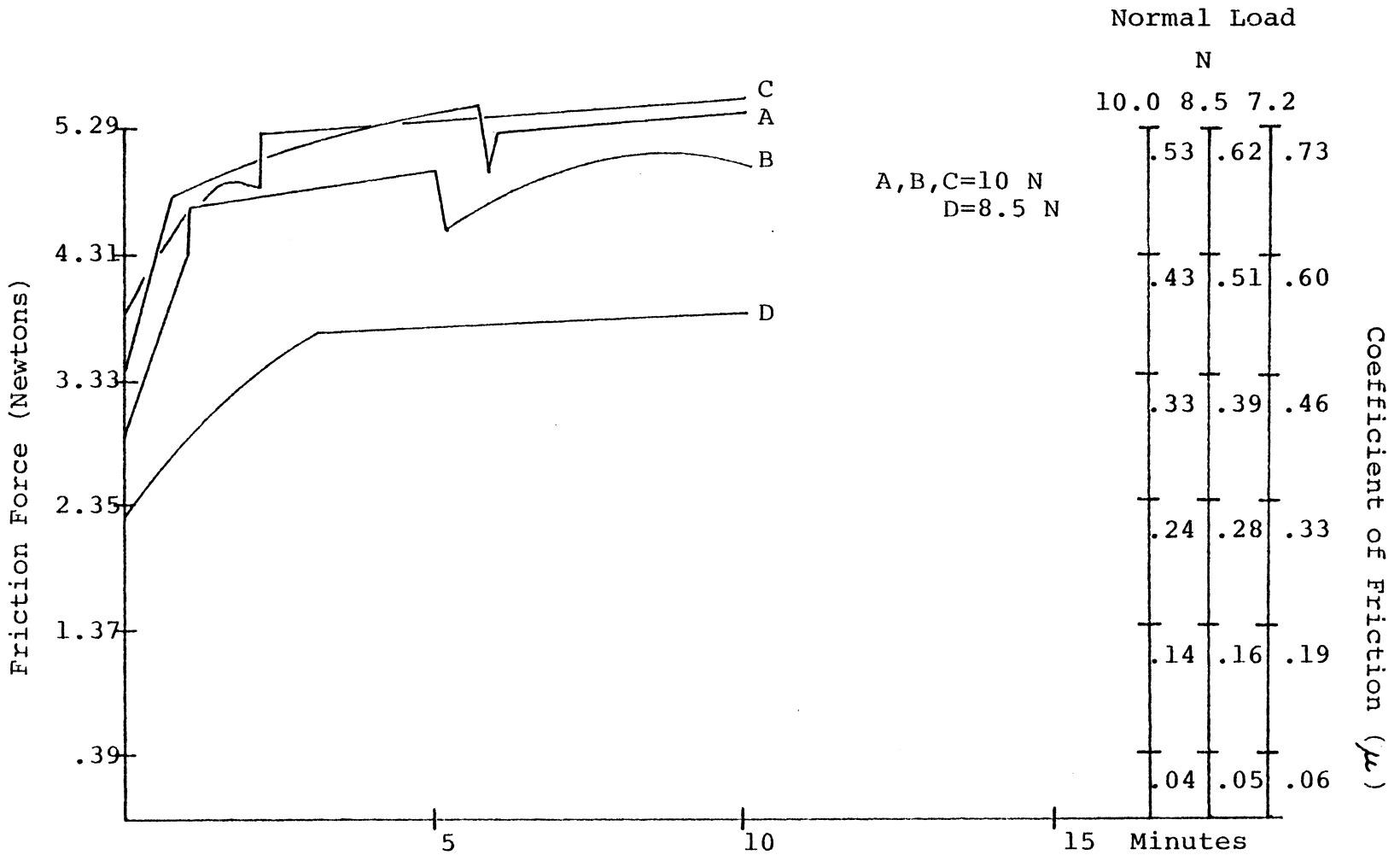

Figure 6A. Friction trace for trial PC IlA-polycarbonate in dry sliding.

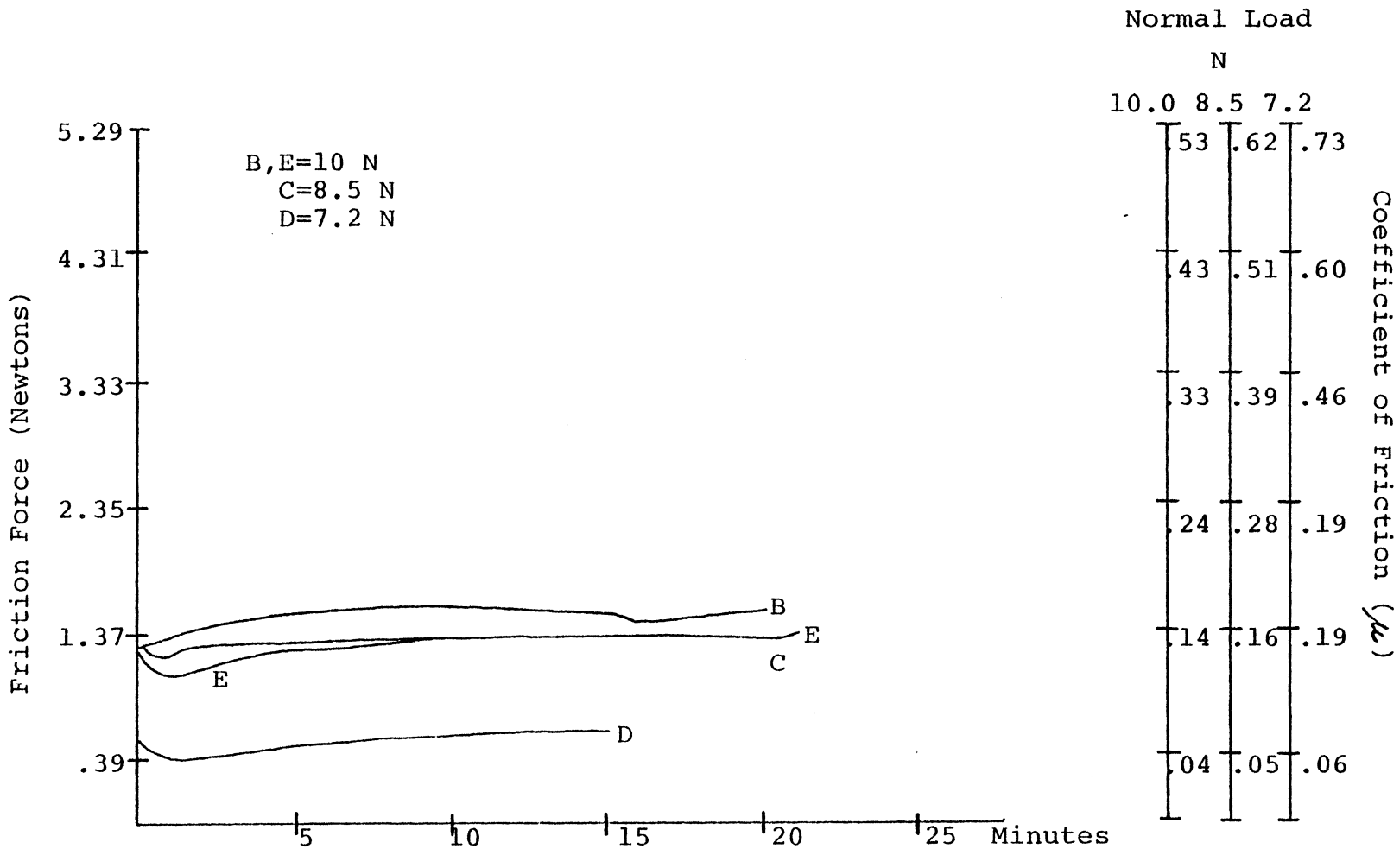

Figure 7A. Friction trace for trial UPE IlA-UHMWPE in dry sliding.

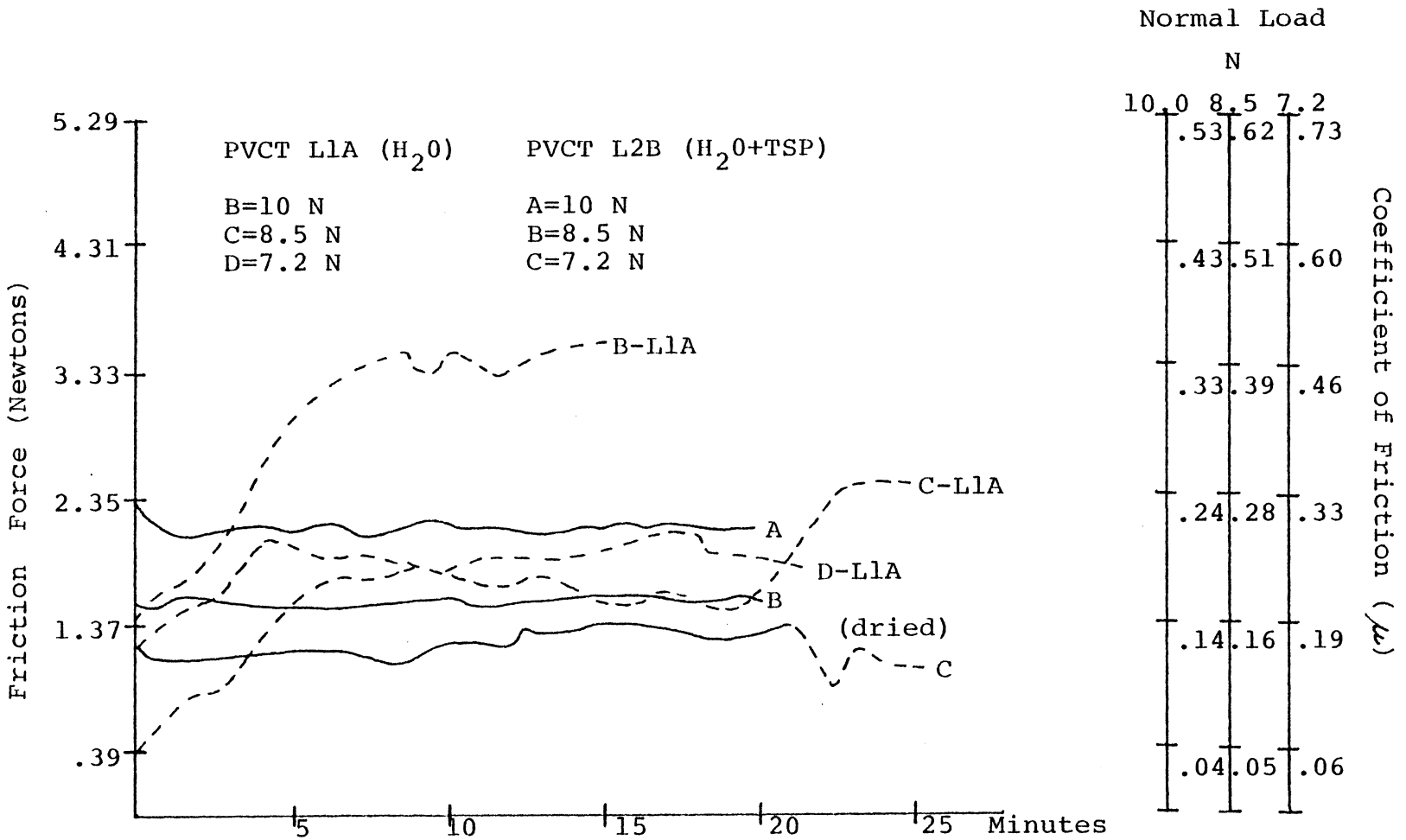

Figure 8A. Friction traces for the H_2O and H_2O+TSP lubrication trial with rigid PVC II.

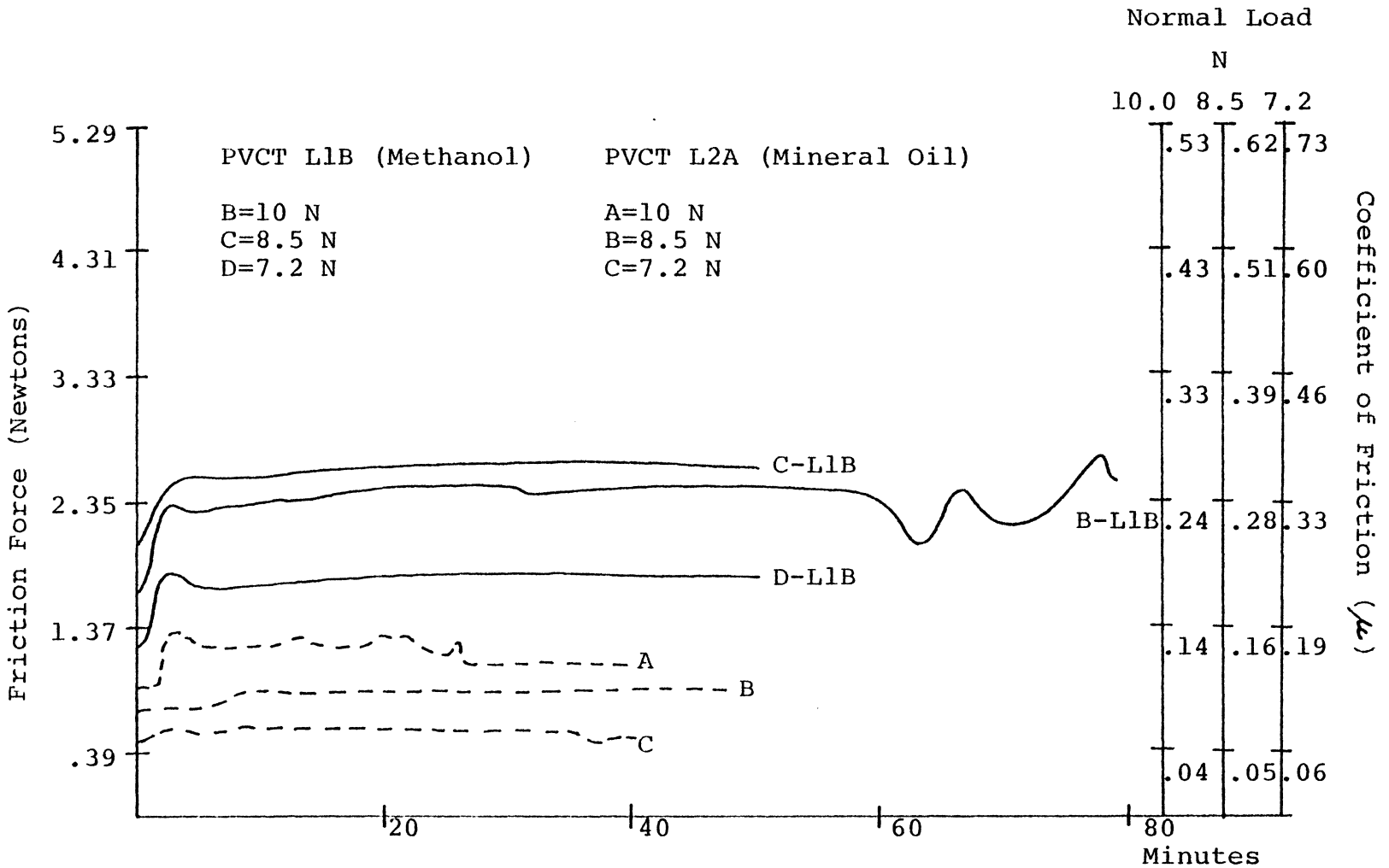

Figure 9A. Friction traces for the methanol and mineral oil lubrication trial with rigid PVC II.

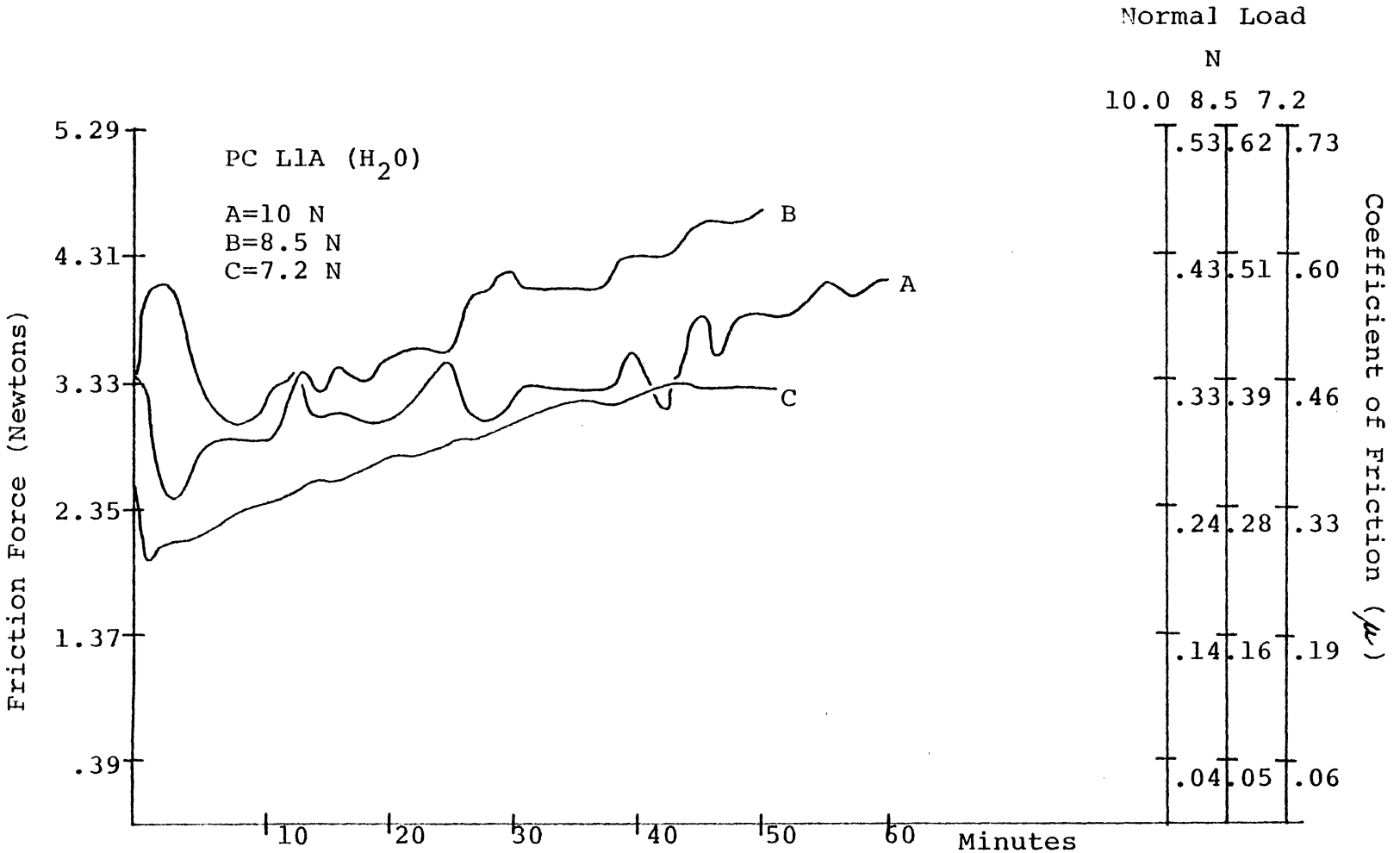

Figure 10A. Friction trace for the H_2O lubrication trial with polycarbonate.

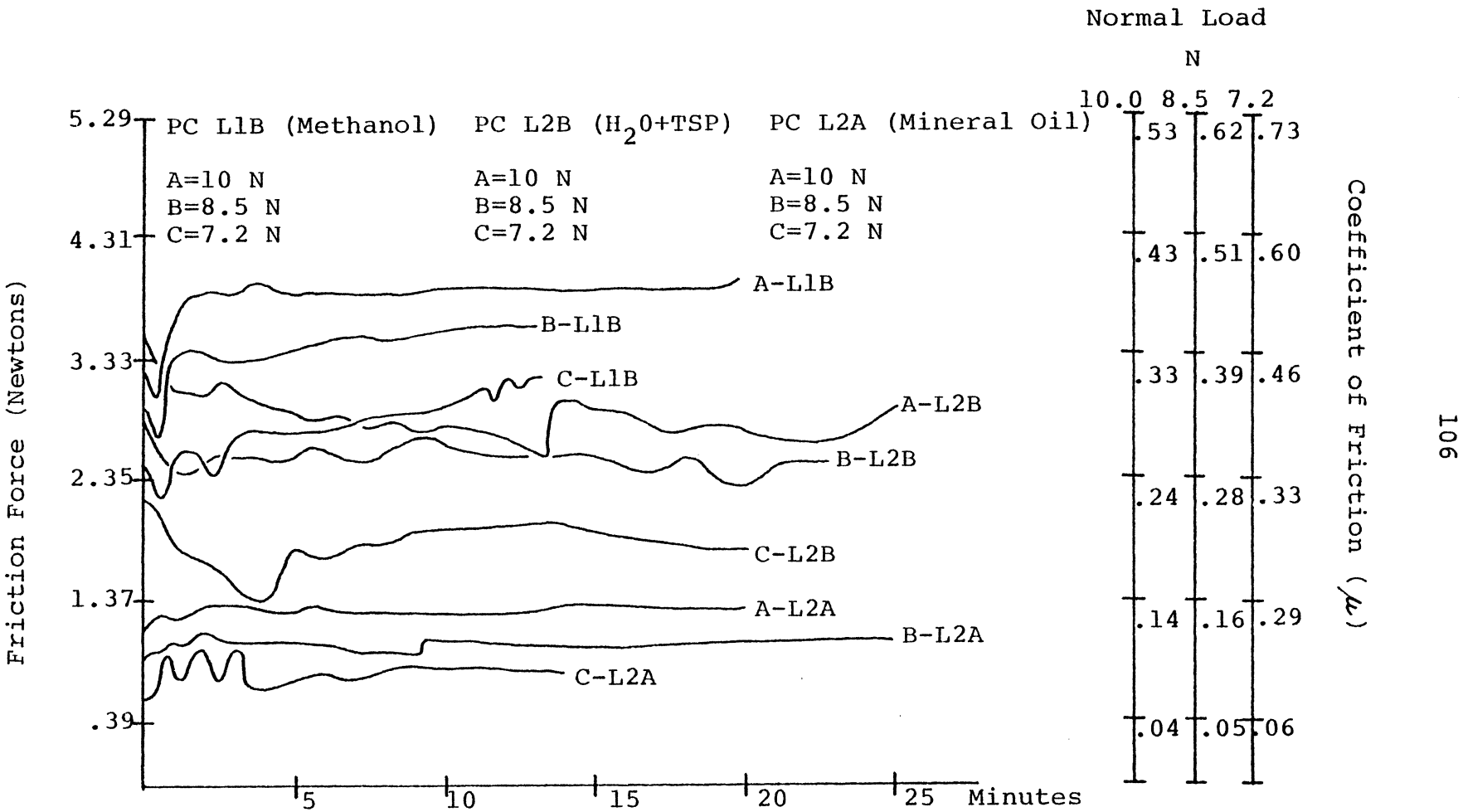

Figure 11A. Friction traces for the $H_2$0+TSP, methanol, and mineral oil lubrication trials with polycarbonate.

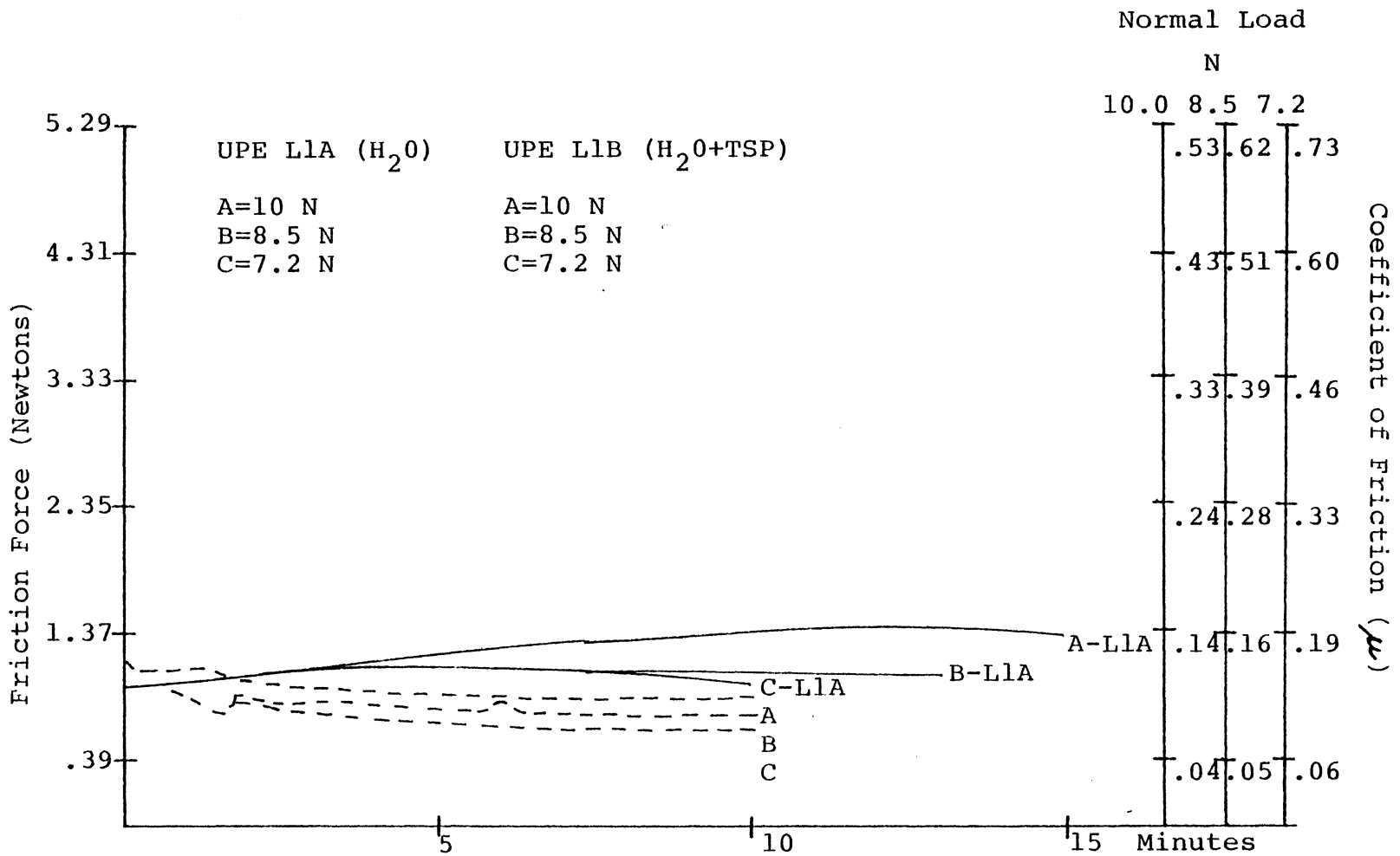

Figure 12A. Friction traces for the H_2O and H_2O+TSP lubrication trials with UHMWPE.

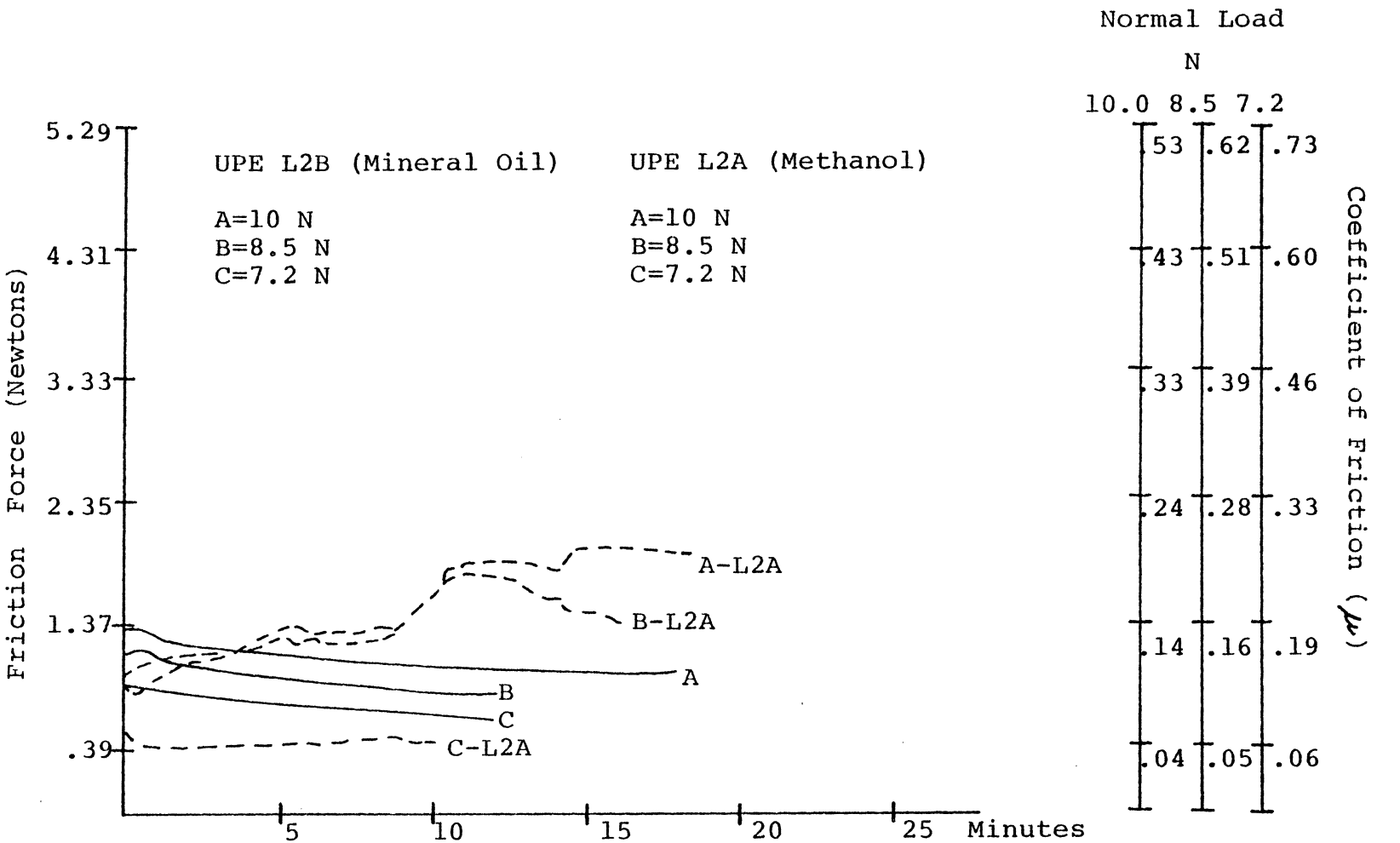

Figure 13A. Friction traces for the methanol and mineral oil lubrication trials for UHMWPE.

APPENDIX B

TRIAL EVENTS

TABLE 7

DATA FOR TRIAL PVCT-I3A

Polymer: PVC II, Lubricant: None, Figure 1A

Normal Load (N)	Track Rad. (mm)	RPM	Time (Min.)	No. of Cycles	Friction Force(N)	Coefficient of Friction	Comments
10.0	20.32	18.8	0:00	0	1.40	.14	Start
			5:00	94	1.60	.16	End Run-in
			18:00	339	1.90	.19	Transition Start
			20:30	386	3.10	.31	Transition End
			21:00	395	2.90	.29	Post Trans. Drop
			22:00	414	2.90	.29	Test Terminated
10.0	19.69	19.4	0:00	0	1.30	.13	Start
			2:30	78	1.50	.15	End Run-in
			14:00	271	1.70	.17	Transition Start
			18:00	349	2.10	.21	Rapid Transition
			19:30	380	3.20	.32	Transition End
			20:00	388	2.80	.28	Post Trans. Drop
			22:00	427	2.90	.29	Test Terminated
8.5	19.05	20.1	0:00	0	1.19	.14	Start
			13:30	271	1.70	.20	Transition Start
			16:00	321	2.60	.31	Transition End
			18:00	361	2.70	.32	Test Terminated
7.2	18.42	20.7	0:00	0	.94	.13	Start
			15:00	311	1.37	.19	Transition Start
			19:00	394	2.16	.30	Test Terminated

TABLE 8

DATA FOR TRIAL PVCT-I4A

Polymer: PVC II, Lubricant: None, Figure 2A

Normal Load (N)	Track Rad. (mm)	RPM	Time (Min.)	No. of Cycles	Friction Force(N)	Coefficient of Friction	Comments
10.0	20.32	18.8	0:00	0	.60	.06	Start
			:30	9	1.10	.11	End Run-in
			1:15	23	1.00	.10	Drop After Run-in
			10:00	188	1.20	.12	Transition Start
			14:45	278	2.40	.24	(a)
			15:00	282	3.00	.30	(b)
			17:00	301	2.50	.25	Test Terminated
10.0	19.69	19.4	0:00	0	.70	.07	Start
			2:00	39	1.00	.10	End Run-in
			8:00	156	1.30	.13	Transition Start
			10:30	204	2.80	.28	(c)
			12:00	233	2.50	.25	Test Terminated
8.5	19.05	20.1	0:00	0	.68	.08	Start
			3:00	60	.89	.11	End Run-in
			10:00	201	1.11	.13	(d)
			17:00	341	2.47	.29	Test Terminated
7.2	18.42	20.7	0:00	0	.57	.08	Start
			4:00	83	.90	.13	End Run-in
			5:00	104	.90	.13	(e)
			17:00	352	2.12	.30	Test Terminated

(a) End Smooth Transition, Debris Observed 14:50
(b) Rapid Transition End
(c) End Transition, Debris Observed 10:00
(d) Transition Start, Wear Track Visible 15:00
(e) Transition Start, Debris Observed 8:00

TABLE 9

DATA FOR TRIAL PVCT-I4B

Polymer, PVC II, Lubricant: None, Figure 3A

Normal Load (N)	Track Rad. (mm)	RPM	Time (Min.)	No. of Cycles	Friction Force(N)	Coefficient of Friction	Comments
10.0	20.32	18.8	0:00	0	.90	.09	Start
			3:00	56	1.20	.12	End Run-in
			9:00	171	1.30	.13	Transition Start
			14:45	277	2.90	.29	Transition End
			15:00	282	2.50	.25	Post Trans. Drop
			16:00	301	2.50	.25	Test Terminated
10.0	19.69	19.4	0:00	0	.70	.07	Start
			4:00	78	1.00	.10	End Run-in
			13:00	253	1.40	.14	Transition Start
			15:50	307	2.90	.29	Transition End
			16:00	311	2.50	.25	Post Trans. Drop
			17:00	330	2.50	.25	Test Terminated
8.5	19.05	20.1	0:00	0	.68	.08	Start
			1:30	30	1.11	.13	End Run-in
			2:00	40	1.01	.12	Drop After Run-in
			5:00	100	1.01	.12	Transition Start
			11:45	235	2.38	.28	Transition End
			12:00	245	2.13	.25	Post Trans. Drop
			13:00	261	2.30	.27	Test Terminated
7.2	18.42	20.7	0:00	0	.43	.06	Start
			2:00	41	.72	.10	End Run-in
			7:00	145	1.37	.19	Transition Start
			14:15	296	1.87	.26	Transition End
			16:00	331	1.87	.26	Test Terminated

TABLE 10

DATA FOR TRIAL PVCO-I4A

Polymer: PVC I, Lubricant: None, Figure 4A

Normal Load (N)	Track Rad. (mm)	RPM	Time (Min.)	No. of Cycles	Friction Force(N)	Coefficient of Friction	Comments
10.0	20.32	18.8	0:00	0	1.20	.12	Start
			6:00	113	1.80	.18	Transition Start
			12:00	226	3.10	.31	Transition End
			17:00	322	3.30	.33	Maximum Friction
			18:00	339	3.20	.32	Test Terminated
10.0	19.69	19.4	0:00	0	1.20	.12	Start
			6:00	116	1.80	.18	Transition Start
			16:00	310	3.40	.34	Transition End
			18:00	349	3.40	.34	
			20.00	388	3.40	.34	Test Terminated
8.5	19.05	20.1	0:00	0	1.03	.12	Start
			6:00	120	1.51	.18	Transition Start
			13:00	260	2.75	.32	First Trans. Peak
			14:00	281	2.47	.29	Transition Drop
			15:15	306	2.92	.34	Transition End
			20:00	400	2.94	.35	Test Terminated
7.2	18.42	20.7	0:00	0	.95	.13	Start
			6:30	135	1.42	.20	Transition Start
			10:30	218	2.17	.30	First Trans. Peak
			12:00	249	2.38	.33	Transition End
			16:00	331	2.43	.34	Test Terminated

TABLE 11

DATA FOR TRIAL PVCO-I5A

Polymer: PVC I, Lubricant: None, Figure 5A

Normal Load (N)	Track Rad. (mm)	RPM	Time (Min.)	No. of Cycles	Friction Force(N)	Coefficient of Friction	Comments
10.0	20.32	18.8	0:00	0	.60	.06	Start
			4:00	75	1.00	.10	End Run-in
			8:00	150	1.20	.12	Transition Start
			10:45	202	2.60	.26	Transition End
			15:00	282	2.60	.26	
			19:00	357	2.60	.26	Test Terminated
10.0	19.69	19.4	0:00	0	.60	.06	Start
			5:00	97	1.00	.10	Transition Start
			13:30	262	2.60	.26	Transition End
			17:00	330	2.80	.28	
			21:00	407	2.80	.28	Test Terminated
8.5	19.05	20.1	0:00	0	.52	.06	Start
			9:30	190	1.01	.12	Transition Start
			16:45	336	2.18	.26	Test Terminated
7.2	18.42	20.7	0:00	0	.53	.07	Start
			10:00	207	.95	.13	Transition Start
			21:00	436	2.02	.28	Test Terminated

TABLE 12

DATA FOR TRIAL PC-I1A

Polymer: Polycarbonate, Lubricant: None, Figure 6A

Normal Load (N)	Track Rad. (mm)	RPM	Time (Min.)	No. of Cycles	Friction Force(N)	Coefficient of Friction	Comments
10.0	20.96	18.2	0:00	0	3.30	.33	Start
			:45	14	4.80	.48	Rapid Trans. End
			5:45	105	5.40	.54	Transition End
			5:55	107	4.90	.49	Post Trans. Drop
			6:00	109	5.30	.53	
			10:00	182	5.40	.54	Test Terminated
10.0	20.32	18.8	0:00	0	2.90	.29	Start
			1:00	19	4.70	.47	Rapid Trans. End
			5:00	94	5.00	.50	
			5:15	99	4.50	.45	Friction Drop
			8:45	166	5.20	.52	Maximum Friction
			10:00	188	5.10	.51	Test Terminated
10.0	19.69	19.4	0:00	0	3.70	.37	Start
			1:45	35	4.90	.47	First Trans.Peak
			2:15	43	4.80	.48	Friction Drop
			2:15	44	5.30	.53	Transition End
			10:00	194	5.50	.55	Test Terminated
7.2	19.05	20.1	0:00	0	2.30	.32	Start
			3:00	60	3.67	.51	Transition End
			10:00	201	3.82	.53	Test Terminated

TABLE 13

DATA FOR TRIAL UPE-I1A

Polymer: UHMWPE, Lubricant: None, Figure 7A

Normal Load (N)	Track Rad. (mm)	RPM	Time (Min.)	No. of Cycles	Friction Force(N)	Coefficient of Friction	Comments
10.0	20.32	18.8	0:00	0	1.30	.13	Start
			9:00	169	1.60	.16	End Run-in
			15:00	282	1.60	.16	
			15:30	293	1.50	.15	Friction Drop
			20:00	376	1.60	.16	Test Terminated
10.0	18.42	20.7	0:00	0	1.30	.13	Start
			:45	17	1.10	.11	Friction Drop
			4:00	83	1.30	.13	Friction Rise
			10:00	207	1.30	.13	
			21:00	435	1.40	.14	Test Terminated
8.5	19.69	19.4	0:00	0	1.36	.16	Start
			:45	14	1.19	.14	Friction Drop
			2:00	39	1.29	.15	Friction Level
			15:30	300	1.41	.17	Friction Peak
			20:00	388	1.29	.15	Test Terminated
7.2	19.05	20.1	0:00	0	.57	.08	Start
			1:00	20	.43	.06	Friction Drop
			10:00	201	.57	.08	Smooth Increase
			15:00	301	.09	.62	Test Terminated

TABLE 14

DATA FOR TRIAL PVCT-L1A

Polymer: PVC II, Lubricant: H_2O, Figure 8A

Normal Load (N)	Track Rad. (mm)	RPM	Time (Min.)	No. of Cycles	Friction Force(N)	Coefficient of Friction	Comments
10.0	19.69	19.4	0:00	0	1.40	.14	Start
			5:00	97	2.90	.29	Rapid Friction
			9:00	173	3.50	.35	First Friction Peak
			12:00	233	3.30	.33	
			15:00	292	3.50	.35	Test Terminated
8.5	19.05	20.1	0:00	0	1.19	.14	Start
			4:30	90	2.04	.42	First Friction Peak
			12:00	240	1.67	.20	Friction Drop
			19:00	383	1.46	.17	End Friction Drop
			22:45	458	2.47	.29	Rapid Friction
			25:00	503	2.47	.29	Test Terminated
7.2	18.42	20.7	0:00	0	.43	.06	Start
			6:30	135	1.72	.24	First Friction Peak
			12:00	249	1.87	.26	Smooth Increase
			18:00	373	2.07	.29	2nd Friction Peak
			21:00	436	1.82	.25	Test Terminated

TABLE 15

DATA FOR TRIAL PVCT-L2B

Polymer: PVC II, Lubricant: H_2O + TSP, Figure 8A

Normal Load (N)	Track Rad. (mm)	RPM	Time (Min.)	No. of Cycles	Friction Force(N)	Coefficient of Friction	Comments
10.0	19.69	19.4	0:00	0	2.40	.24	Start
			1:45	34	2.10	.21	Initial Drop
			10:00	194	2.20	.22	
			20:00	388	2.20	.22	Test Terminated
8.5	19.05	20.1	0:00	0	1.62	.19	Start
			:45	15	1.51	.18	Initial Drop
			2:00	40	1.62	.19	
			10:00	201	1.51	.18	
			20:00	402	1.51	.18	Test Terminated
7.2	18.42	20.7	0:00	0	1.18	.16	Start
			1:00	21	1.09	.15	Initial Drop
			12:00	249	1.09	.15	Stable Trace
			12:30	259	1.32	.18	Rapid Increase
			21:00	436	1.37	.19	End Stable Trace
			25:00	519	1.04	.14	Test Terminated

TABLE 16

DATA FOR TRIALS PVCT-L1B AND L2A

Polymer: PVC II, Lubricant: Methanol (L1B) and Mineral Oil (L2A), Figure 9A

Normal Load (N)	Track Rad. (mm)	RPM	Time (Min.)	No. of Cycles	Friction Force(N)	Coefficient of Friction	Comments
10.0	19.69	19.4	0:00	0	1.70	.17	Start(Methanol)
			2:30	49	2.40	.24	Rapid Increase
			55:00	1067	2.50	.25	End Stable Trace
			63:30	1232	2.10	.21	Max. Friction Drop
			79:00	1533	2.50	.25	Test Terminated
			0:00	0	.90	.09	Start(Mineral Oil)
			2:30	49	1.40	.14	Rapid Increase
			26:00	505	1.10	.11	End Friction Drop
			40:00	776	1.10	.11	Test Terminated
8.5	19.05	20.1	0:00	0	1.97	.23	Start(Methanol)
			4:00	80	2.57	.30	Rapid Increase
			50:00	1005	2.61	.31	Test Terminated
			0:00	0	.71	.08	Start(Mineral Oil)
			10:00	201	.89	.11	End Unstable Region
			46:00	922	.89	.11	Test Terminated
7.2	18.42	20.7	0:00	0	1.23	.17	Start(Methanol)
			2:00	41	1.82	.25	Rapid Increase
			50:00	1037	1.82	.25	Test Terminated
			0:00	0	.57	.08	Start(Mineral Oil)
			40:00	830	.53	.07	Test Terminated

TABLE 17

DATA FOR TRIAL PC-L1A

Polymer: Polycarbonate, Lubricant: H_2O, Figure 10A

Normal Load (N)	Track Rad. (mm)	RPM	Time (Min.)	No. of Cycles	Friction Force(N)	Coefficient of Friction	Comments
10.0	19.69	19.4	0:00	0	3.80	.38	Start
			1:30	29	4.20	.42	1st Friction Peak
			9:00	175	2.90	.29	1st Friction Drop
			13:00	252	3.40	.34	2nd Friction Peak
			25:00	485	3.50	.35	3rd Friction Peak
			45:00	873	3.80	.38	4th Friction Peak
			60:00	1164	4.10	.41	Test Terminated
8.5	19.05	20.1	0:00	0	3.32	.39	Start
			3:00	60	2.43	.29	Friction Drop
			6:00	120	2.89	.34	1st Friction Peak
			13:30	271	3.42	.40	2nd Friction Peak
			30:00	603	4.18	.49	3rd Friction Peak
			50:00	1005	4.66	.55	Test Terminated
7.2	18.42	20.7	0:00	0	2.56	.36	Start
			1:00	21	1.92	.27	Friction Drop
			42:00	871	3.27	.45	Friction Peak
			51:00	1058	3.27	.45	Test Terminated

TABLE 18

DATA FOR TRIAL PC-L2B

Polymer: Polycarbonate, Lubricant: H_2O + TSP, Figure 11A

Normal Load (N)	Track Rad. (mm)	RPM	Time (Min.)	No. of Cycles	Friction Force(N)	Coefficient of Friction	Comments
10.0	19.69	19.4	0:00	0	3.60	.36	Start
			:45	15	3.00	.30	Friction Drop
			2:30	49	3.20	.32	1st Friction Peak
			13:30	262	2.50	.25	End Friction Drop
			13:45	267	3.00	.30	2nd Friction Peak
			25:00	485	3.00	.30	Test Terminated
8.5	19.05	20.1	0:00	0	2.85	.34	Start
			1:30	30	2.38	.28	Friction Drop
			2:00	40	2.57	.30	1st Friction Peak
			9:00	181	2.75	.32	2nd Friction Peak
			23:00	460	2.57	.30	Test Terminated
7.2	18.42	20.7	0:00	0	2.22	.31	Start
			3:30	73	1.37	.19	Friction Drop
			4:45	99	1.82	.25	1st Friction Peak
			13:00	270	2.02	.28	Max. Friction
			20:00	415	1.82	.25	Test Terminated

TABLE 19

DATA FOR TRIAL PC-L1B

Polymer: Polycarbonate, Lubricant: Methanol, Figure 11A

Normal Load (N)	Track Rad. (mm)	RPM	Time (Min.)	No. of Cycles	Friction Force(N)	Coefficient of Friction	Comments
10.0	19.69	19.4	0:00	0	3.20	.32	Start
			:30	10	3.00	.30	Friction Drop
			1:15	24	3.90	.39	Friction Peak
			20:00	388	4.00	.40	Test Terminated
8.5	19.05	20.1	0:00	0	2.99	.35	Start
			:30	10	2.66	.31	Friction Drop
			1:30	30	3.42	.40	Friction Peak
			13:00	260	3.62	.43	Test Terminated
7.2	18.42	20.7	0:00	0	2.52	.35	Start
			:30	11	2.17	.30	Friction Drop
			1:30	31	2.66	.37	1st Friction Peak
			2:15	47	2.47	.34	Friction Drop
			3:30	73	2.80	.39	2nd Friction Peak
			13:15	275	3.17	.44	Test Terminated

TABLE 20

DATA FOR TRIAL PC-L2A

Polymer: Polycarbonate, Lubricant: Mineral Oil, Figure 11A

Normal Load (N)	Track Rad. (mm)	RPM	Time (Min.)	No. of Cycles	Friction Force(N)	Coefficient of Friction	Comments
10.0	19.69	19.4	0:00	0	1.20	.12	Start
			2:30	49	1.40	.14	Friction Peak
			20:00	388	1.40	.14	Test Terminated
8.5	19.05	20.1	0:00	0	.94	.11	Start
			2:00	40	1.17	.14	Friction Peak
			25:00	503	1.06	.12	Test Terminated
7.2	18.42	20.7	0:00	0	.67	.09	Start
			:45	16	1.09	.15	Peak Unstable
			3:15	67	.72	.10	End Unstable Trace
			14:00	290	.81	.11	Test Terminated

TABLE 21

DATA FOR TRIALS UPE-L1A AND L1B

Polymer: UHMWPE, Lubricants: H_2O (L1A) and H_2O + TSP (L1B), Figure 12A

Normal Load (N)	Track Rad. (mm)	RPM	Time (Min.)	No. of Cycles	Friction Force(N)	Coefficient of Friction	Comments
10.0	19.69	19.4	0:00	0	1.00	.10	Start(H_2O)
			11:00	213	1.40	.14	Max. Friction
			15:00	291	1.40	.14	Test Terminated
			0:00	0	1.30	.13	Start(H_2O + TSP)
			2:00	39	1.00	.10	Friction Drop
			10:00	194	.90	.09	Test Terminated
8.5	19.05	20.1	0:00	0	.85	.10	Start(H_2O)
			5:00	100	1.08	.13	Max. Friction
			13:00	261	1.08	.13	Test Terminated
			0:00	0	1.19	.14	Start(H_2O + TSP)
			1:30	30	.75	.09	Friction Drop
			1:45	35	.89	.11	1st Friction Peak
			6:00	120	.89	.11	2nd Friction Peak
			10:00	201	.75	.09	Test Terminated
7.2	18.42	20.7	0:00	0	.90	.13	Start(H_2O)
			5:00	104	1.23	.17	Max. Friction
			10:00	207	.99	.14	Test Terminated
			0:00	0	1.23	.17	Start(H_2O + TSP)
			5:00	104	.72	.10	
			10:00	207	.72	.10	Test Terminated

TABLE 22

DATA FOR TRIAL UPE-L2A

Polymer: UHMWPE, Lubricant: Methanol, Figure 13A

Normal Load (N)	Track Rad. (mm)	RPM	Time (Min.)	No. of Cycles	Friction Force(N)	Coefficient of Friction	Comments
10.0	19.69	19.4	0:00	0	1.10	.11	Start
			5:00	97	1.30	.13	1st Friction Peak
			9:00	175	1.40	.14	Rapid Increase
			11:00	213	1.90	.19	2nd Friction Peak
			14:00	272	1.90	.19	Friction Increase
			15:00	291	2.10	.21	3rd Friction Peak
			19:00	369	2.00	.20	Test Terminated
8.5	19.05	20.1	0:00	0	.94	.11	Start
			:30	10	.85	.10	Friction Drop
			5:00	100	1.36	.16	1st Friction Peak
			7:30	150	1.19	.14	Friction Drop
			10:30	211	1.79	.21	2nd Friction Peak
			16:00	322	1.41	.17	Test Terminated
7.2	18.42	20.7	0:00	0	.57	.08	Start
			:45	16	.48	.07	Friction Drop
			5:00	104	.48	.07	
			8:45	181	.57	.08	1st Friction Peak
			10:00	207	.48	.07	Test Terminated

TABLE 23

DATA FOR TRIAL UPE-L2B

Polymer: UHMWPE, Lubricant: Mineral Oil, Figure 13A

Normal Load (N)	Track Rad. (mm)	RPM	Time (Min.)	No. of Cycles	Friction Force(N)	Coefficient of Friction	Comments
10.0	19.69	19.4	0:00	0	1.30	.13	Start
			:30	10	1.40	.14	1st Friction Peak
			1:00	19	1.30	.13	Friction Drop
			9:00	175	1.20	.12	
			18:00	349	1.10	.11	Test Terminated
8.5	19.05	20.1	0:00	0	1.13	.13	Start
			:45	15	1.20	.14	Friction Peak
			1:30	30	1.02	.12	Friction Drop
			12:00	240	.92	.11	Test Terminated
7.2	18.42	20.7	0:00	0	.94	.13	Start
			6:00	124	.78	.11	
			12:00	248	.65	.09	Test Terminated

The vita has been removed from the scanned document